Journal of Nanotechnology

Nanocomposites 2013

Guest Editors: Hongmei Luo, John Zhanhu Guo, Menka Jain, Ping Xu, and Guifu Zou

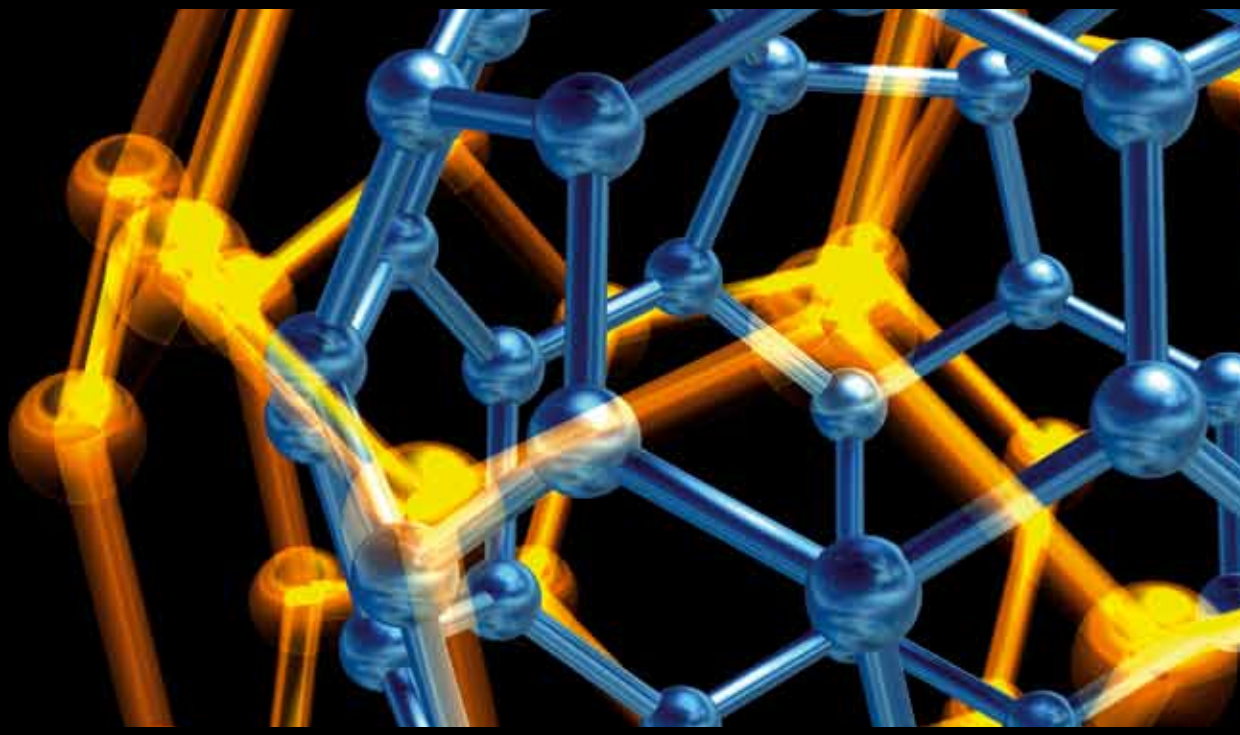

Nanocomposites 2013

Journal of Nanotechnology

Nanocomposites 2013

Guest Editors: Hongmei Luo, John Zhanhu Guo, Menka Jain, Ping Xu, and Guifu Zou

Editorial Board

Contents

Hindawi Publishing Corporation
Journal of Nanotechnology
Volume 2013, Article ID 856143, 1 page
http://dx.doi.org/10.1155/2013/856143

Editorial
Nanocomposites 2013

Hongmei Luo,[1] John Zhanhu Guo,[2] Menka Jain,[3] Ping Xu,[4,5] and Guifu Zou[6]

[1] *Department of Chemical Engineering, New Mexico State University, Las Cruces, NM 88003, USA*
[2] *Dan F. Smith Department of Chemical Engineering, Lamar University, Beaumont, TX 77710, USA*
[3] *Department of Physics, University of Connecticut, Storrs, CT 06269, USA*
[4] *Department of Chemistry, Harbin Institute of Technology, Harbin 150001, China*
[5] *Chemistry Division, Los Alamos National Laboratory, Los Alamos, NM 87545, USA*
[6] *School of Energy, Soochow University, Suzhou 215000, China*

Correspondence should be addressed to Hongmei Luo; hluo@nmsu.edu

Received 30 October 2013; Accepted 30 October 2013

Composite materials that traditionally incorporate micron-scale reinforcements in a bulk matrix offer opportunities to tailor material properties such as hardness, tensile strength, and thermal and electrical conductivity. With the advent of nanomaterials, nanocomposites are multiphase materials where one of the phases has at least one dimension of less than 100 nm. The properties of nanocomposite materials depend not only on the properties of the building components but also on their morphologies, microstructures, and interfacial characteristics. The published works are briefly addressed as follows.

The paper from Canada reports that dispersion, microstructure, and dielectric response of polyethylene (PE)/clay nanocomposites were affected by the incorporation of anhydride modified polyethylene (PE-MA) as the compatibilizer. It was observed that the relaxation rate of the Maxwell-Wagner-Sillars process increased as the degree of dispersion increased. This correlation shows that broadband dielectric spectroscopy can be used as a macroscopic tool to evaluate the quality of dispersion in nanocomposite materials.

The paper from Egypt studies the rheological behavior of a different concentration of carbon nanotubes (CNTs) as additive on lithium grease under various settings of shear rate, shear stress, and apparent viscosity. The authors concluded that the optimum percentage of CNTs in the grease composite was 2% and further confirmed the importance of the correlation between rheological properties and the grease microscopic structure.

Another paper from India is about the biological synthesis of silver nanoparticles (AgNPs) using cannonball leaves. Such AgNPs showed cytotoxicity to human breast cancer cell line (MCF-7). Overall, this environment-friendly method of biological Ag nanoparticles production can potentially be used in various human contacting areas such as cosmetics, foods, and medical applications.

The other paper in this issue, also from India, is about the mechanical properties and thermal conductivity investigation of epoxy resin by dispersion multiwalled carbon nanotubes (MWCNTs) in the composites. It was found that the compressive strength, Young's modulus, and thermal conductivity of composites with MWCNTs were increased compared to those of pure epoxy. By comparison with different methods, the paper concluded that a unique method for the dispersion of MWCNTs in epoxy is the solvent dispersion technique with vacuum drying process.

Hongmei Luo
John Zhanhu Guo
Menka Jain
Ping Xu
Guifu Zou

Hindawi Publishing Corporation
Journal of Nanotechnology
Volume 2013, Article ID 641581, 16 pages
http://dx.doi.org/10.1155/2013/641581

Research Article

Some Fundamental Aspects of Mechanics of Nanocomposite Materials and Structural Members

Alexander N. Guz and Jeremiah J. Rushchitsky

S. P. Timoshenko Institute of Mechanics, Nesterov Street 3, 03680 Kiev, Ukraine

Correspondence should be addressed to Jeremiah J. Rushchitsky; rushch@inmech.kiev.ua

Received 24 June 2013; Accepted 6 September 2013

Academic Editor: Ping Xu

This paper is devoted to formulation and analysis of fundamental aspects of mechanics of nanocomposite materials and structural members. These aspects most likely do not exhaust all of the possible fundamental characteristics of mechanics of nanocomposite materials and structural members, but, nevertheless, they permit to form the skeleton of direction of mechanics in hand. The proposed nine aspects are described and commented briefly.

1. Introduction

The specificity of mechanics as science consists in that it is one of the most important sciences of fundamental character and at the same time its urgency is defined by significance for engineering of many problems of mechanics. At all of the stages of human progress, starting with the ancient world, the importance of mechanics for engineering cannot be overemphasized: in many cases, mechanics, and engineering were considered as a single whole. This specificity of mechanics is shown up, when the mechanics of materials was formed as the scientific direction, in which uniting of mechanics and engineering is very significant.

Mechanics of materials as the direction has been clearly formed in the last century within the framework of solid mechanics along with mechanics of structural members, when the investigations related to the development of new materials were essentially extended. Actually, the sufficiently ponderable part of investigations, which are carried out on solid mechanics, is represented in mechanics of materials. This situation resulted in that in some universities solid mechanics is included in different courses on material science.

On the whole, investigations on mechanics of materials are defined or characterized by the fact that the information on *internal structure of material* is always taken into account, although in different extent. In the most part of investigations on mechanics of materials, this information is used for characterization or identification of materials. In this case, the internal structure is considered in analysis of photo of internal structure and its change under force and technological actions only. In the slightly less part of investigations on mechanics of materials, information on internal structure is included in the models of materials and is utilized in the statement and solution of corresponding problems of mechanics of materials. This allows to separate *the structural mechanics of materials* as the independent scientific direction within the framework of mechanics of materials [1, 2].

Thus, the structural mechanics of materials is meant to be the part of investigations on mechanics of materials, in which the internal structure of materials is taken into account in quantitative and qualitative sense, *when the models of materials are being constructed and the corresponding problems are being studied*.

When structural mechanics of materials is defined in such a way, then the object of its study is the large class of modern materials, including *reinforced concrete*, internal structures of which is defined by presence of armature; *metals, alloys, and ceramics*, internal structure of which are defined by presence of grains and other structural components; *composite materials*, internal structures of which are defined by presence of granules, fibers, and layers; and *nanocomposites*, internal structures of which are defined by presence of nanogranules, nanofibers, and nanolayers.

In this paper, "*macromechanics, mesomechanics, micromechanics, and nanomechanics of materials* are the component parts of *structural mechanics of materials* [1–3]."

The corresponding notions and definitions to the four component parts mentioned above are comparatively established and widely used. The one only and necessary common requirement for all four scientific directions is to take into account the internal structure of material in mechanical models and in solving the corresponding problems.

Below, the proposed fundamental aspects of mechanics of nanocomposite materials and structural members permit to form the skeleton of this direction of mechanics. Introducing the term *structural members* has the goal of considering the following nanocomposite materials object of mechanics, because this object is prevailing in engineering. But relating the structural composite elements to the ones of nanolevels imports the additional restrictions on analysis within the framework of nanomechanics. Furthermore, the above-mentioned aspects are considered sequentially.

2. Aspect 1: Analysis of Internal Structure and Structural Levels

An analysis of internal structure in materials and usage of the notion of structural levels give the straight track to differing the nanomechanics from macro-, meso-, and micromechanics. This notion arose in micromechanics, but it became very productive and maybe the most important for description of nanomechanics, too.

To characterize quantitatively the internal structure of materials as objects of study in structural mechanics of materials, it is expedient to introduce *the geometrical parameter h*.

(i) In the case of reinforced concrete, the parameter h characterizes the mean value of minimal diameters of cross-section of metallic armature.

(ii) In the case of metals, alloys, and ceramics, the parameter h characterizes the mean value of minimal sizes of cells, grains, and other structural inhomogeneities.

(iii) In the case of composite materials with polymeric and metallic matrices, the parameter h characterizes the mean value of minimal diameters of grains for materials of granular structure, the mean value of minimal diameters of cross-sections of fibers for fibrous materials, and the mean value of minimal thickness of layers of components for layered materials.

(iv) In the case of nanomaterials (nanocomposites), the parameter h characterizes the mean value of minimal diameters of nanoparticles or nanolayers.

It seemed to be appropriate to propose *the limits of changing the parameter h*, which determine relating the corresponding materials to macromechanics, mesomechanics, micromechanics, or nanomechanics. It is necessary to note that some scientists proposed variants of changing the parameter h-levels of changing of h. As a consequence of analysis

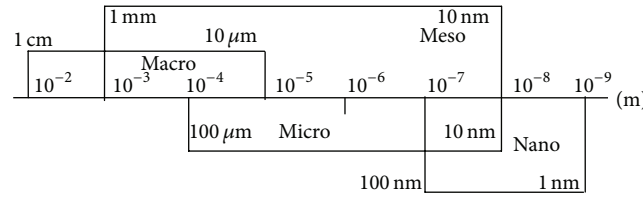

Figure 1: Structural levels.

of proposals of different authors, the next four levels for parameter h were proposed in publications [4, 5]:

$$\text{macro}, 10^{-2}\,\text{m} \geq h \geq 10^{-5}\,\text{m}; \quad \text{meso}, 10^{-5}\,\text{m} \geq h \geq 10^{-7}\,\text{m};$$
$$\text{micro}, 10^{-7}\,\text{m} \geq h \geq 10^{-8}\,\text{m}; \quad \text{nano}, 10^{-8}\,\text{m} \geq h \geq 10^{-9}\,\text{m}. \tag{1}$$

Let us note that the atom level (distance between atom planes in crystal lattice) has the order of one or more angstroms (10^{-10} m); therefore, the nanolevel in (1) is conditionally bounded by 10^{-9} m.

For the convenience of readers, the relationships between used length units are shown as follows:

$$\text{meter, m}; \quad \text{centimeter, cm} = 10^{-2}\,\text{m};$$
$$\text{millimeter, mm} = 10^{-3}\,\text{m}; \quad \text{micron, } \mu\text{m} = 10^{-6}\,\text{m}; \tag{2}$$
$$\text{nanometer, nm} = 10^{-9}\,\text{m}; \quad \text{angstrom, Å} = 10^{-10}\,\text{m}.$$

Attention on that proposed in (1) four levels for parameter h do not overlap one another. In development of some scientific directions related to macro-, meso-, micro- and nanomechanics, the investigations are carryied out in the framework of scale levels, which overlap one another that is, the four level are considered in the extended interpretation.

Based on analysis of proposals of different authors, within the above mentioned extended interpretation the four levels for parameter h were proposed in publications [4, 5]

$$\text{macro}, 10^{-2}\,\text{m} \geq h \geq 10^{-5}\,\text{m}; \quad \text{meso}, 10^{-3}\,\text{m} \geq h \geq 10^{-8}\,\text{m};$$
$$\text{micro}, 10^{-4}\,\text{m} \geq h \geq 10^{-8}\,\text{m}; \quad \text{nano}, 10^{-7}\,\text{m} \geq h \geq 10^{-9}\,\text{m}. \tag{3}$$

Schematically, four levels (3) are shown in Figure 1 [1, 2, 4, 5].

Thus, within the framework of this aspect, the tool of identification of the material as the nanomaterial is generated.

3. Aspect 2: Modeling in Mechanics of Nanocomposite Materials and Structural Members

Constructing the mechanical models can be thought as the main goal of mechanics. Let us remember the well-known sentence of Truesdell's [6]: *in fact, mechanics is an infinite class of models to represent certain aspects of nature*. Mechanics of materials, of course, is understood as part of mechanics

and can be meant as exploring the infinite set of mechanical models of materials. Usually, the mechanical models are related to the theoretical part of mechanics and are formulated in terms of mathematics and physics. Nowadays, the theoretical models consist of the structural and mathematical parts, but, traditionally, they are meant as the mathematical models. Each theoretical model in mechanics underlies, as a rule, the corresponding mechanical theory.

The models of materials are by their sense some idealizations of the real materials, and applicability of every model should be tested. Thus, the experimental mechanics presents the special part of mechanics and forms the fundamental knowledge, which arises owing to direct contact with real nature (in solid mechanics, with real materials). For fundamental sciences, the necessity of attention to experiments and practice had been formulated far back by Leibniz in his statement "*theoria cum practica*." Today, it is understood as the necessity for any theory to amplify with experimentations. 200 years later, Boltzmann stated "*nothing is so practical as the theory.*" In 1926, in a talk between Werner von Heisenberg and Albert Einstein, Heisenberg stated that each theory, in its building, must correspond to only those observed by this time facts. Einstein answered that it could be wrong to try to build the theory only on observed facts. Really, it happens the *vice versa*. Theory determines, what we can observe.

So, when the process of deformation of materials is being described (modeled), then different models are applied taking into account the discrete structure of material at the atom level and not taking into account this structure within the framework of continuum representation.

Note that the continuum representation of material consists in that real piece of material (material body) is replaced by continuum of the same geometrical shape. In each point of continuum, the values of physical-mechanical parameters of material (physical-mechanical properties) and physical-mechanical fields (stresses, strains, temperature, and so on) are considered.

The following three types of media are studied:

(i) *homogeneous media* (continua), when values of physical-mechanical parameters (constants) do not depend on the point (they are one and the same for all of the medium);

(ii) *piecewise homogeneous media* (continua), consisting of separate parts of homogeneous media, which are continuously jointed and form one continuum;

(iii) *inhomogeneous media* (continua) with continuously changing inhomogeneity.

The main advantage of continuum description consists in that it permits to apply the methods of continuous mathematics and, in particular, the differential and integral calculi. At present, owing to active development of the finite element method and discrete mathematics, the significance of continuum representation will be possibly refined.

Among the above mentioned models, the following principally distinguished models should be marked out as such, which are the most widespread ones.

Model 1: the model of discretely arranged rigid particles (which model the atoms), interacting with themselves.

Model 2: the model of piece-wise continuous body, each component of which is described within the framework of continuum representation.

Model 3: the model of homogeneous body, which is analyzed within the framework of continuum representation.

In *solid physics*, the investigations are carried out within the framework of crystal lattice concept, that is, within the framework of *model 1*, in which interaction among atoms is put into effect by interatomic interaction forces caused by potentials of different structure. Such approach is represented in a number of monographs, among which it seems that the quite actively cited monograph [7] should be pointed, and in plentiful publications in scientific journals.

In particular, the model exists for discretely arranged rigid particles (balls), placed at nodes of crystal lattice and jointed by springs. In this case, the interaction among neighbouring balls is realized by the link of their springs. This model is used in mechanics, too. As an example, the monograph [8] can be pointed out, in which this model is applied to study dynamical processes occurring in the fracture wave.

In *micromechanics of composite materials*, the investigations are carried out within the framework of *model 2*—the model of piece-wise homogeneous body, consisting of separate particles of the filler (reinforcing elements) and the binder (matrix). Description of deformation of each particle of the filler and the matrix is done within the framework of continuum representation. In this model, the interaction among separate particles of the filler is realized through the continuous body (matrix) by means of condition of continuity of stress and displacement vectors at the filler-binder interface. On the interface, the different variants of joining the filler and the binder can occur in some materials, which is reflected in changing the concrete form of conditions of continuity. Such an approach is represented in a row of monograph editions ([9–20] and others) and in the large number of journal publications (e.g., [21, 22]).

Model 3—the model of homogeneous body with averaged properties—is successfully used in mechanics of composite materials. At that, the body is assumed frequently to be anisotropic. Then, in the most part of cases, composites are assumed to be orthotropic ones. The same model is used in mechanics of structural elements (shells, plates, rods, and so on) made of composite materials. It is described in many monographs and original papers [23–49]. Usually, in macro- and mesomechanics, only models 2 and 3 are used, since on this scale level the components of composite material are the sufficient big pieces of real material. The problem of discrete structure of the piece is already not actual. It is worthy to note that for model 2 the homogenization can be required.

Undoubtedly, the essential part of investigations in mechanics of structural members is referring to the case when through the thickness the member consists of several homogeneous anisotropic layers. In these investigations,

the two-dimensional (for shells and plates) and one-dimensional (for rods) applied theories are mainly considered, which are constructed by introduction of hypotheses on distribution of stresses and displacements through the thickness.

Above, three models are considered comparatively briefly. These models along with other models are everywhere applied in structural mechanics of materials. Each of the models has its possibilities, advantages, disadvantages, when in mechanics of materials the concrete phenomena are being described, and specific difficulties in the realization.

Probably, the most complex model from the point of view of obtaining the concrete results is the second one—the model of piecewise homogeneous body. Let us show in support two reasons.

Reason 1 consists in that within the framework of this model each reinforcing element is studied within the framework of continuum mechanics-solid mechanics, which is developed very well.

Reason 2 consists in that interaction of different reinforcing elements occurs through the matrix, which is also studied within the framework of continuum mechanics-solid mechanics and permits therefore to use plenty of analytical approaches.

In mechanics of composite materials, three models discussed above as well as many other models are applied to composite materials in the form of the sequence (chain) of models, which provide at the final stage the study within the structural members made of these composite materials. This reflects the specificity of mechanics as science.

Obviously, the sequences (chains) of used models for different composite materials, and studied within them, phenomena are different too, because the level scales (1) and (3) and Figure 1 should be taken into account. So, for nanocomposites, models 1, 2, and 3 are included into the sequence, whereas for macro-, meso- and microcomposites, only models 2 and 3 are inculded.

When mechanics of composite materials are being constructed in the sense noted above, then different approaches and methods are utilized, which correspond to different scientific directions and scientific positions of single scientists. Nevertheless, despite such diversity of scientific directions, in construction of mechanics of composite materials, *two basic principles* (two basic concepts) are applied on *principle of continualization and principle of homogenization*, which are formulated below.

The principle of continualization consists in

> "*that the discrete system is changed (modeled) by the continuous system (medium) and for the continuous system (medium) the corresponding averaged properties are determined*."

This principle is used widely, for example, within the framework of model 1 in transition to the continuum theory of dislocations in crystal lattices.

The principle of homogenization consists in "*changing (modeling) the piece-wise homogeneous system, deforming the elements (pieces) of which is described by the relationships of continuum mechanics of solids, by the homogeneous continuous system (medium), and by the determination of necessary averaged properties within the framework of the homogeneous continuous system (medium)*."

The principle of homogenization is widely used within the framework of model 2 in micromechanics of composite materials, when different problems of statics, dynamics, stability, and fracture are being studied.

Usually, the area which a continuously inhomogeneous body (e.g., a composite material with the continuous changing in some direction number of micro- or nanospheres) or piece-wise homogeneous body (e.g., a composite material with uniformly distributed micro- or nanospheres by all of the directions) occupies is chosen, dimensions of which are essentially of less body sizes. This area should contain the sufficiently large number of inhomogeneities (e.g., granules) to provide the averaging correctness. Such an area is called *the representative volume*.

The averaged properties of the volume are usually attributed to the point at the volume center. As a result, the averaged properties are evaluated at every point of the body, and these properties should be constant—the body becomes the homogeneous one.

Very often, authors of different publications on materials are showing the color pictures of representative volumes in the form of cubes filled of discrete particles, which are looking very nice but do not image as a rule the real discrete structure.

The representative volume side length is compared with the characteristic length of body internal structure or with the characteristic length of inhomogeneities in the body (e.g., with micro- or nanosphere diameter). Exceeding the first length over the second one one order or more gives grounds to apply the averaging procedure.

Let us note that, from the abovestated continualization and homogenization principles, their principled distinction and methodological commonality follow (especially, in relation to the initial systems, to which they are applied).

Let us note finally that the procedures of continualization and homogenization are realized by means of different methods of averaging. At that, as a rule, the notion of representative volume is used.

Furthermore, three basic moments in realization of modeling with using the notion of representative volume and methods of averaging will be pointed.

Moment 1. When the notion of representative volume, which will be later denoted as V_{Π}, is being introduced, it is assumed that the minimal linear sizes of volume V_{Π} are significantly more than the maximal sizes of discrete particles (in case of *model 1*) or maximal sizes of homogeneous parts of material (in case of *model 2*). Thus, the linear sizes of representative volume must be significantly more introduced before the geometrical parameter h.

Usually, the majority of authors are assuming that exceeding the first value over the second value on one or more orders gives grounds for the next modeling and averaging.

Parallel to selection of the representative volume V_{Π} (which is separated in the initial model: *model 1 or 2*), select the equivalent volume V_E also within the framework of

the final model: the model of homogeneous body (*model 3*). *Assume* that volume V_Π has the same shape as volume V_E and is oriented in the same way. In this regard, the following denotation is used frequently:

$$V_\Pi = V_E = V. \tag{4}$$

Moment 2. When the material is being modeled (the values and parameters in the equivalent volume V_E being determined by means of averaging through corresponding values and parameters in the representative volume V_Π), it *is assumed* that the only homogeneous fields of stresses, strains, and so on are arising in the equivalent volume

$$\left\langle \sigma_{ij} \right\rangle = \text{const}_{ij}, \qquad \left\langle \varepsilon_{nm} \right\rangle = \text{const}_{nm}, \ldots. \tag{5}$$

It is expedient to stress that only in the analysis situations, corresponding to conditions (5), the possibility exists to determine the averaged values of different parameters (constants), which are included within the constitutive equations for homogeneous material (*the model 3*). At that, the methods of averaging are used for different quantities.

Consider as an example the procedure of determination of potential energy of deformation of elastic body in volumes V_Π and V_E, for which corresponding denotations E_Π and E_E will be introduced. Also, denote by $\Phi(\varepsilon_{ij})$ the specific potential energy of deformation of elastic material with internal structure (model 1 or 2), which is referred to as the unit of volume V_Π and in which the components of the Green strain tensor according to model 2 or 3 are denoted as ε_{ij}. In his case, for volume V_Π, the following formula is valid:

$$E_\Pi = \int_{V_\Pi} \Phi\left(\varepsilon_{ij}\right) dV_\Pi. \tag{6}$$

For volume V_E (in which the stress and strain fields are already homogeneous), the energy can be evaluated too as following:

$$E_E = \left(\int_0^{\langle \varepsilon_{ij} \rangle} \left\langle \sigma_{ij} \right\rangle d \left\langle \varepsilon_{ij} \right\rangle \right) V_E. \tag{7}$$

In the case of linearly elastic body, the following expression for volume V_E can be obtained from formula (7) as follows:

$$E_E = \left(\frac{1}{2}\right) \left(\left\langle \sigma_{ij} \right\rangle \left\langle \varepsilon_{ij} \right\rangle \right) V_E. \tag{8}$$

From (4) and (8), for the material with volume V in different modeling from the initial model (*model 1 or 2* in volume V_Π) to the final model (*model 3* in volume V_E), when potential energy of elastic deformation is being averaged, the relationships can be written as

$$\left\langle \sigma_{ij} \right\rangle \left\langle \varepsilon_{ij} \right\rangle = \frac{2}{V} \int_V \Phi\left(\varepsilon_{nm}\right) dV. \tag{9}$$

It is necessary to note that, along with expression (8), in carrying out the operation of averaging and evaluation of values of averaged parameters (constants), similar expressions are used, which follow from conditions of equilibrium for different structural components in V_Π and from conditions of their common deformation.

Moment 3. The results of modeling and averaging, within the framework of approaches discussed in *moments 1 and 2*, are applicable in description of stress, strain, and other fields, which change insignificantly on distances of the same order as sizes of the representative volume V_Π.

If the stated, in description of moment 1, reasons on determination of the linear sizes of the representative volume V_Π through the introduced before geometrical parameter h are taken into account, then the following conclusion can be achieved.

> "*The results of modeling and averaging from above are applicable in description of stress, strain, and other fields which change insignificantly on distances exceeding one order or more the value of geometrical parameter h*."

Note that, in the practical realization of averaging procedure, the majority of authors are assuming additionally that in the material structural components (within the framework of the representative volume V_Π) the homogeneous fields of stresses, strains, and other quantities are realized (different for filler and binder). Such an approach simplifies essentially evaluation of integrals of the type of the right side of expression (8).

Thus, the shown description of aspect 2 can be related to arguments about similarity of all four parts of structural mechanics of materials, because all of the continuum mechanics models of these parts are identical.

4. Aspect 3: Only Two Basic Models

The feature of composite materials is their forming from the binder (matrix) and fillers (reinforcing elements). When composites as materials with the clearly shown internal structure are modeled, a row characterizing this structure geometrical parameters should be known.

Of course, when the approaches and methods of mechanics of composite materials of any level of internal structure are developed, one cannot orient the geometrical parameter h only, because it determines a place of the composite in the hierarchical structure of materials only. It is necessary to take into account the character of mechanical processes under consideration.

In this regard, the geometrical parameter L is introduced, which characterizes the variability of mechanical fields by spatial coordinates. Also, it turned out to be expedient to introduce for nanoformations the geometrical parameter h^*, which characterizes the mean value of distances between centers of particles in the internal structure of nanoformation.

The introduced parameters L, h, and h^* enable the determination of two essentially different models and corresponding methods of their analysis within the framework of mechanics of composite materials.

Model 1. This model is the piecewise homogeneous medium or model of discrete particles. It is applied when parameter L is the quantity of the same order or less as compared with the parameters h, h^* characterizing the structure of composite material. This condition can be represented by use of some inequalities as follows

$$L \approx h, \quad L < h, \quad L \approx h^*, \quad L < h^*. \tag{10}$$

If at least one of conditions (10) is fulfilled, then deformation of matrix and reinforcing elements is described by relationships of the continuum solid mechanics under some conditions at interfaces, which correspond to conditions of continuity of stress and displacement vectors.

When the 3D relationships of continuum solid mechanics are used, this approach is the most exact and rigorous within the framework of continuum solid mechanics. Using this model, the investigations of problems of statics, dynamics, stability, and fracture in mechanics of composite materials are carried out. If at least one of conditions (10) is fulfilled when applied to a nanoformation, then the motion of this nanoformation is described by relationships of the model of discrete particles.

Model 2. This model is the piecewise homogeneous anisotropic body with averaged properties. It is utilized when the characterizing of a variability of mechanical fields by the spatial variables parameter L which is the quantity more essentially than the characterizing of the structure of composite materials parameters h, h^*. This condition can be written in the form of inequalities

$$L \gg h, \quad L \gg h^*. \tag{11}$$

In this case, a composite material is modeled by the homogeneous anisotropic body with averaged properties. Some intermediate criteria between (10) and (11) can be formulated, but they will be of less importance when comparing with (10) and (11). For example, in the case of pure filling (very small volume fraction of fillers), the mean value of minimal diameters of fillers h is essentially smaller than the value of distance among the filler centers h^*; that is, $h \ll h^*$. But the condition $L \gg h^*$ still must be saved.

At present, the theoretical and experimental methods of determination of averaged constants are elaborated for composite materials in the framework of this model. Especially, the progress in development of theoretical methods should be emphasized.

Model 2 is obtained as the result of utilization of the homogenization principle. Let us remember that it consists in changing the piece-wise homogeneous continuum by some homogeneous continuous continuum with the corresponding averaged properties within the framework of the model of anisotropic medium.

Finally, it seems to be expedient to note that *model 2* is more approximate when comparing with *model 1*. Therefore, the exactness of results obtained by *model 2* can be estimated using the results obtained by *model 1*.

Let us stop on some perspectives of developing based on model 2 approach. First of all, discreteness of structure of nanoformations as mechanical systems is of common knowledge. Also, when physical-mechanical properties of nanoformations are being determined, the concept of *continualization* is as a rule applied, and the discrete structure is approximately changed by a homogeneous continuous system (continuum). At that, the quantities are determined, which are peculiar for the continuum solid mechanics (Young modulus, Poisson ratio, proportional limit, yield strength, ultimate strength, corresponding to fracture strains, and so forth). Of course, in most cases of analysis of nanomaterials, the use of principle of continualization seems to be expedient, too.

Taking into account the insufficient level of studying the properties of nanoformations and the existence of, at present, quite good base of mechanical characteristics of microcomposite materials, let us adduce first the necessary facts from micromechanics of materials for the following comparative discussion. Among many important achievements of micromechanics of composite materials, let us show only two.

The first achievement is related to understanding the role of mechanical models: one and the same composite can be described by diverse microstructural models: from the complex multicontinuum models to the discrete models in the form of lattices [50–53]. Every model has some advantages, when either concrete problem is studied. The plenty of models testifies the achieved depth of understanding in micromechanics of materials.

The second achievement consists in that there is the big set of different mechanical characteristics for components of composite materials (matrixes, granules, fibers, and layers).

Below, as an example, the list for such set for aramid fibers (kevlars) is shown [54]:

> "*(1) density; (2) diameter of single fiber; (3) equilibrium humidity; (4) ultimate strength under tension; (5) elongation under break; (6) initial elastic modulus; (7) maximal elastic modulus; (8) elastic modulus under bending; (9) calculation modulus under axial tension; (10) dynamical elastic modulus; (11) part of strength in the loop from the ultimate strength under tension; (12) fatigue properties (number of cycles up to failure); (13) creep under loading up to 90% of the ultimate strength; (14) constant of friction*."

At present, the information on mechanical characteristics of nanoformations is still insufficient, and the listed above example with fourteen characteristics of certain fiber can be understood as the very distant goal in nanomechanics.

Thus, aspect 3 can be, like aspect 2, related to arguments about similarity of all four parts of structural mechanics of materials, because two basic models of the continuum mechanics of these parts are identical.

5. Aspect 4: Allowance for the Edge and Near-the-Surface Effects

The problem of allowance for the edge and near-the-surface effects is important for all of the parts of mechanics of materials. As a rule, analysis of this problem permits to estimate the validity of continuum models.

Remember that, in structural mechanics of composites (in the broad sense) and in mechanics of composite materials (in the more narrow sense), the principles of continualization and homogenization are utilized. According to the first one, the discrete structure is changed (modeling) by the continuous structure. According to the second one, the piecewise homogeneous structure is changed (modeling) by the homogeneous structure.

It is necessary to take into account that principles of continualization and homogenization are referring to modeling the properties of material as the infinite continuum.

When different problems of structural mechanics of materials (problems of statics, dynamics, stability, and fracture) are being studied, analysis is necessary to be carried out as a rule for the material occupying the finite volume, which is also characterized by the boundary surface. On the boundary surface, for all of the basic mechanical processes, some boundary conditions are formulated for the material. In this regard, the question on applicability of principles of continualization and homogenization near the boundary surface and on this surface arises. The answer to this question can be formulated as follows:

> "*near the boundary surface, the principles of continualization and homogenization do not work*."

The proof of this statement seems to be quite evident, because near the boundary surface (under loading of arbitrary type) the representative volume of material is inherent in this material basic property-property of *homogeneity* of fields of macrostresses and macrostrains. The macrostresses and macrostrains are understood here as the stresses and strains within the framework of continuous system (medium), to which the initial system is reduced after application of continualization and homogenization principles.

Note also that, in composite materials, when the material is being modeled by the piecewise homogeneous medium, the inhomogeneous fields of stresses and strains near the boundary surface in each component (each homogeneous medium) arise as a rule. The statement above is true for all of the four scales mechanics (macro-, meso-, micro-, and nano-).

Below, inapplicability of principles of continualization and homogenization near the boundary surface is illustrated by an example of layered materials within the framework of micromechanics of composite materials. More specifically, let us consider the layered composite material formed of two alternating layers of constant thickness, which are made of materials with distinguishing properties.

In Figures 2 and 3, the two-dimensional representative area is shown, which includes the part of boundary surface also, that is, the representative volume near the boundary surface. At that, the dotted line denotes the exarticulation of the part of material near the boundary surface, and the size of the representative area side is $10(h_1 + h_2)$, where h_1 and h_2 are the thicknesses of the forming of material layers. Thus, the sizes of representative area are distinguished one order from the structural components size $(h_1 + h_2)$, which usually, in different publications, is assumed to be sufficient, when the sizes of representative area are being discussed.

It seems obvious that, owing to presence of boundary surface with arbitrary sizes of the representative area in Figures 2 and 3, the strains and stresses in the representative area are inhomogeneous. At that, this inhomogeneity will decrease with distance from the boundary surface. This phenomenon of inhomogeneity of fields is known in solid mechanics for *homogeneous materials*. In this case, the values of strains and stresses become more homogeneous, when moving off from the boundary surface.

When applied to statical problems, this phenomenon corresponds to the Saint-Venant edge effect.

When applied to problems of wave dynamics, this phenomenon corresponds to onset of surface waves with amplitude damping with moving off from the boundary surface.

The notion of surface instability for homogeneous anisotropic body (which corresponds to *model 3*) is seemingly introduced for the first time in [55]. Results of investigations of phenomenon of surface instability for different homogeneous materials with using strong 3D theories are represented along with other results in many monographs (e.g., starting with [56, 57] and finishing with [58, 59]). In the work in [60], the phenomenon occurring near the boundary surface of elastic anisotropic body was called *the skin effect*.

Thus, in problems of statics, dynamics, and stability of mechanics of homogeneous materials (including *model* 3), the phenomenon consisting in the fields of inhomogeneous strains and stresses arising near the boundary surface of material, which damp quickly moving off from the boundary surface (skin effect, edge effect, and near-the-surface effect), is known quite well.

It is obvious that similar type effects take place both for materials with discrete structure (*model 1*) and for piece-wise homogeneous materials (*model 2*). For these materials, owing to existence of edge or near-the-surface effects, the additional complication arises-*near the boundary surface*, the principles of continualization and homogenization are inapplicable, because, including the boundary surface representative volume of arbitrary size, the fields of strains and stresses are *inhomogeneous*.

Taking into account the considerations above, it seems expedient to form the following conclusions.

Conclusion 1. For materials with discrete structure (*model 1*) and for piece-wise homogeneous materials (*model 2*), the study of edge effects can be carried out within the framework of initial models only because the principles of continualization and homogenization are here inapplicable.

Conclusion 2. For the convenience of studying, the edge and near-the-surface effects can be divided on effects near

the boundary surface, which is parallel to the direction of prevailing reinforcement (the shown type in Figure 2), and effects near the boundary surface of the end face type are perpendicular to the direction of prevailing reinforcement (the shown type in Figure 3).

Conclusion 3. Analysis of edge and near-the-surface effects can be carried out within the model of homogeneous anisotropic body (*model 3*) also, but the results will be spurious as compared with analysis within the framework of *models 1 and 2*.

At present, a row of results is obtained in studying the edge and near-the-surface effects of the shown type in Figures 2 and 3 they are obtained within the framework of the model of piece-wise homogeneous material (*model 2*). The results are obtained for the model that corresponds to Conclusion 1.

Note that the strong method of solving the problems on near-the-surface effects in the case when the boundary surface is parallel to interfaces is proposed in the monograph [61] when applied to the layered materials of periodic structure. Here, the edge and surface effects are studied within the framework of wave dynamics: the propagation of surface waves along the plane boundary.

When applied to edge effects in the case when the boundary surface is perpendicular to interfaces in layered or fibrous materials, the results of studying the static problems of materials are stated in [9–20]. Here, only the simplest problems are studied, and the results are obtained using the numerical methods.

For the near-the-surface effects, when the boundary surface is parallel to interfaces, the results on constructing the surface instability of layered materials are stated in [57]. Here, for cases of the full contact of layers and the sliding layers, the method proposed in [61] was used. For the case of presence of cracks at interface, the numerical methods were used. These results correspond to fracture mechanics under compression, when the initial stage of fracture is the stability loss in the near-the-surface layers.

For the near-the-surface effects in fibrous unilateral composites, when the boundary surface is parallel to fibers, the results on constructing the surface instability are stated in [57]. These results correspond to fracture mechanics of fibrous materials under compression, when the initial stage of fracture is the stability loss of fibers in the near-the-surface area.

Let us show finally the exceptional example of composite material, in which the type of loading and the structure of composite are such that the edge and near-the-surface effects shown in Figures 2 and 3 do not arise. Consider a layered composite material composed of orthotropic layers of constant thickness. Layers differ by thickness and physical-mechanical properties. Symmetry axes of materials of layers coincide with the coordinate axes. So, the layered composite with arbitrary number of layers in the package is analyzed. Such a package is shown in Figure 4. It is assumed that at interfaces the conditions of continuity of displacement and stress vectors are fulfilled. The shown analysis rests valid for other boundary conditions at interfaces.

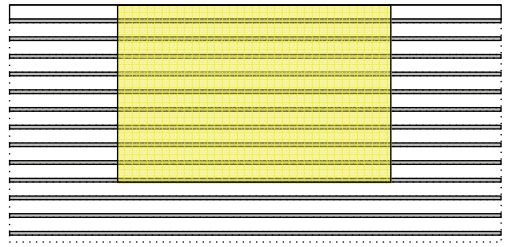

Figure 2: The layered material with boundary surface parallel to interfaces.

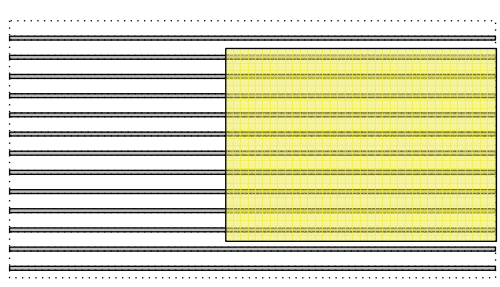

Figure 3: The layered material with boundary surface placed perpendicularly to interfaces.

The case of plane strain in the plane x_1Ox_2 is considered, when compression along the axis Ox_1 is realized by the rigid discs, which are shown in Figure 4 by rectangles of black color. It is assumed that the rigid discs provide the identical for all the layers shortening and the possibility of slipping motion of end faces of each layer along discs. Then, in each layer, the homogeneous stress-strain state is arising, different for different layers. In this way, the edge effects of the two above-considered types do not arise.

Note that at the end face of each layer the following boundary conditions $u_1 = Cx_1$ (C = const) and $\sigma_{12} = 0$ are given. If the compression is realized by the uniformly distributed normal load, then within the framework of the plane strain state the edge effects near the end face will already arise.

The similar phenomenon of absence of edge effects arises also in the fibrous unilateral composite materials under their compression through the rigid discs along the reinforcing fibers. This phenomenon of homogeneous stress-strain state in the matrix and the fibers arises, when additionally assuming the coefficient of transverse expansion of the matrix and the fibers to be identical.

The shown above discussion of the edge and near-the-surface effects forms a separate aspect of structural mechanics of materials, which provides the best understanding of results, which are obtained by means of principles of continualization and homogenization. This aspect testifies similarity of all four parts of structural mechanics of materials, including the nanomechanics of materials.

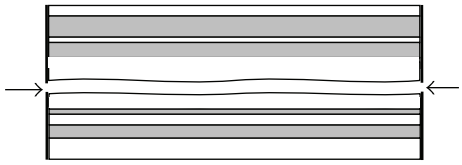

Figure 4: Layered composite material composed of orthotropic layers of constant thickness.

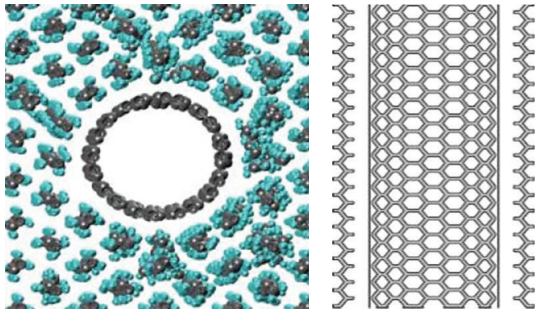

Figure 5: The molecular structure of nanocomposite crystallic polyethylene—CNT.

6. Aspect 5: Phenomena at Interface in Nanocomposite Materials

These phenomena arise in all of the kinds of composite materials and are studied very intensively. To analyze such phenomena, it seems convenient to introduce the notion of *geometrical interface* of nanoformation and polymeric matrix.

> "*The geometrical interface is meant to be the surface, sizes, and shape which are determined when nanoformations are being described in continuum approximation*."

When the nanoformations and matrix are united into a nanocomposite, the phenomena occur at interfaces with participation of more deep-laid mechanisms that take place, for example, in the case of microcomposites.

The point is that in the general case the nanoformations consist of a system of curvilinear layers; in turn, each layer consists of a system of atoms, interaction among which is determined by force of interatomic interaction.

Therefore, when the nanoformations and matrix are being composed into a nanocomposite, seemingly, the interaction of atoms of the "end" layer of atoms on nanoformation with the neighboring atoms of polymeric matrix must occur owing to forces of interatomic interaction.

Thus, some intermediate layer arises from materials of nanoformations and polymeric matrix, inside which the interaction of atoms of nanoformations and polymeric matrix is observed. For example, in Figure 5, the molecular structure of nanocomposite *crystallic polyethylene—CNT*—is shown schematically.

Note that Figure 5 corresponds to [62] and is modified here to illustrate existence of intermediate layer discussed above. On the left side of Figure 5, the cross-section of nanocomposite is shown.

Let us note also that studying this phenomenon and finding the characterizing regularities seem to be the complex and urgent physical-chemical problem. The solution of this problem can be realized by representatives of corresponding scientific directions only.

To describe the phenomena in the intermediate layer within the framework of mechanics of nanocomposites in cases like those shown above, it is expedient to use the traditional approaches of mechanics developed early, when the related problems are being considered.

The tradition in mechanics in an analysis of phenomena occurring in the intermediate thin layers or on surfaces of thin bodies consists in

> "*modeling these phenomena by certain boundary conditions*."

At that, the *boundary conditions are transferred* on certain in some sense close but the simpler surface.

Consider the following few examples.

Example 1. In the classical theory of wing flow, the boundary conditions on the wing surface are *transferred* on the wing chord.

Example 2. In the classical theory of contact interaction of elastic bodies, in the case when the stamp bottom has some deviations from the plane form, the boundary conditions are *transferred* on the plane boundary.

Example 3. In the problem of dynamical interaction of fluid and elastic (including thin-wall) bodies, the boundary conditions on vibrating interface are *transferred* at the fixed interface.

Taking into account these traditional, in mechanics approaches and practice of modeling of nanoformations and matrix by continuum systems, the following, corresponding to and adopted in mechanics, exactness approach can be proposed:

> "*it is expedient to model the phenomena occurring in the thin intermediate layer (nanoformation + polymeric matrix) by certain boundary conditions of interfacing of two media and translating these conditions at the geometrical interface "nanoformation matrix"*".

This approach has been proposed at the first time, seemingly, in [62].

Ascertainment of concrete structure of boundary conditions, reflecting the phenomena in intermediate layer, is still problematic, because physicists and chemists still have not built the sufficiently grounded theory of such phenomena.

Because establishing the concrete structure of boundary conditions at geometrical interface seems to be problematic, the development of bilateral estimates for these conditions becomes of special urgency. Such estimates permit to estimate also the values of corresponding quantities.

From the point of view of mechanics, the most *stiff* or *perfect* interfacing of two media (in this case, interfacing of

the nanoformation and matrix) in the continuum description corresponds to the *conditions of total contact* (continuity of stress and displacement vectors) at the interface; the most compliant or imperfect interfacing of two media corresponds to the *conditions of sliding contact*.

Thus, *the study of nanocomposites under two mentioned types of boundary conditions at geometrical interface enables to obtain the bilateral estimates for quantities of interest*, when various physical-chemical mechanisms are being manifested at the interface.

It should be also stressed that numerous problems exist in mechanics of microcomposites that are associated with necessity to provide the corresponding adhesion strength at interface. These problems are arising because of the existence of various mechanisms at interface. But these mechanisms in microcomposites are not linked with the interatomic forces action, contrary to nanocomposites, in which this action can be essential.

7. Aspect 6: The Validity Ranges of Continuum Mechanics of Materials

Such an aspect exists in every physical theory. It forms the necessary element in the theory and, of course, should be discussed when applied to the structural mechanics of materials. Below, the reasons and information are expounded, arising in analysis of the validity ranges of continuum mechanics of materials.

Let us note that undoubtedly the strong and full solution of the problem of validity ranges is difficult to realize from mathematical point of view. In this regard, *below, it is only one among many variants of its approximate solution and qualitative discussion that is considered*.

Remember that, in mechanics of composite materials, the basic relationships of continuum mechanics of materials are used to describe the deformation of matrix and each reinforced element. Note also that validity of continuum mechanics of materials in cases of macro-, meso-, and micromechanics is analyzed quite well. Here, the case of nanomechanics is discussed.

Return now to relationships (1) and (3) and Figure 1; from which it follows that the structural nanomechanics studies the materials, in which the reinforcing particles can reach sizes not less than 1 nm. At that, the distance between the atom planes has as a rule the order of one or more angstroms. It is accepted that atoms have also diameters of the order of angstrom.

The typical example of the filler used to produce the nanocomposites is *the carbon nanotube*—single-walled (SWCNT) or multiwalled (MWCNT) [63]. It is well known that the SWCNT is the carbon molecular layer, consisting of ordered (zig-zag, armchair, and chiral) structure of carbon atoms, which is as if rolled into the cylindrical tube. From the point of view of molecular physics, the carbon nanotube is the discrete system consisting of particles (atoms) the sizes of which have the order of 1.5 angstrom; at that, the distance between particles reaches the order of 1 nm. Interaction among elements of this discrete system (among carbon atoms) is put into effect by nonmechanical way, because the material medium among separate carbon atoms is absent. Interaction among neighboring carbon atoms in the one atom layer (SWCNT) as well as the interaction among carbon atoms in neighboring layers (MWCNT) is put into effect by the forces of interatomic interaction, which is described by different potentials.

At present, in overwhelming number of theoretical publications, to determine the properties of carbon nanotubes, the approaches of molecular structural physics are used. They are based on the Cauchy-Born method [7] with using a different potential, describing the interatomic interaction (e.g., potentials in the Brenner form [64], Tersoff-Brenner form [65, 66], modified Morse potential [67], and so on).

As a result of such approaches, the peculiars for continuum solid mechanics quantities are obtained: the values of Young modulus, Poisson ratio, and others. In this way, the continualization of discrete system is realized, when the interaction among single elements (single atoms) occurs owing to forces of interatomic interaction.

Note that attempt to describe the deformation of reinforcing elements, especially nanotubes, within the framework of continuum solid mechanics, seems to be perspective and probably *solely expedient*, because it must correlate with description of deformation of matrix, for which the continuum approach is peculiar.

Taking into account the abovementioned, the problem of validity of basic relationships of continuum solid mechanics in the study of mechanical processes on the nanolevel (3) can be formulated as follows.

Which mechanical fields can be studied on the nanolevel (3)*, assuming the system in hand as the continuum or applying the basic relationships of continuum solid mechanics*?

At that, it should be noted that the mechanical fields (stress and strain fields) in a nanoformation (e.g., in the nanotube) change by spatial variables.

Introduce, therefore, *the geometrical parameter* L, which characterizes the mechanical processes (characterizes the variability of mechanical fields by spatial variables) and has the dimension of length. In the case of statical problems, the parameter L corresponds to the minimal distances, on which the stress and strain fields change significantly; in the problems of wave propagation, the parameter L corresponds to the wavelength, and in the stability problems it corresponds to the wavelength of stability loss mode.

Thus, the problem of validity ranges is equivalent to the problem of determination of ranges for parameter L, which provide possibility to study the mechanical fields on the nanolevel (3) using the basic relationships on continuum solid mechanics (i.e., assuming the discrete system in hand as the continuum and homogeneous one).

To solve this problem, it seems necessary to use the introduced before and the characterized internal structure of material geometrical parameter h. Also, the geometrical parameter h^* seems expedient to be introduced. It characterizes the mean value of distances between centers of particles in the internal structure of material.

Taking into account the information above on atom sizes and distances between atoms, it can be assumed that parameters h and h^* have, when applied to nanoformations the following values:

$$h \approx 1.5 \text{ angstrom}, \qquad h^* \approx 1 \text{ nm}. \tag{12}$$

The values in (12) can be chosen in a different way. For example, the value $h \approx 1.5$ angstrom corresponds to the carbon atom diameter.

Qualitative and partially quantitative solutions of the problem under consideration can be carried out by introducing the model of anisotropic homogeneous body. It is necessary for applicability of this model that the parameter L (characterizing the variability of mechanical fields by the spatial variables) by more essentially quantity as compared with parameters h and h^* (characterizing the structure of composite material). This situation is provided by fulfilling the following conditions:

$$L \gg h, \qquad L \gg h^*. \tag{13}$$

So, it follows from (12) and (13) that mechanical fields on nanolevel can be studied with utilization of the basic relationships of continuum solid mechanics, if the geometric parameter L meets the condition

$$L \gg 1 \text{ nm}. \tag{14}$$

If the condition "$\gg$" (more essentially) is fulfilled when the quantities are distinguished even on one order, then condition (14) can be represented in the form

$$L \geq 10 \text{ nm}. \tag{15}$$

Thus, when the mechanical fields, for which the parameter L fulfills either condition (14) or (15), are being studied, the model of continuum can be used (or the basic relationships of continuum solid mechanics can be used, which in this case is identical) for nanocomposite materials taking into account their real atom structure.

The condition (14) or (15) determines the validity ranges of continuum solid mechanics in studying the mechanical fields in composite material components (i.e., separately in the matrix material and separately in the material of each reinforcing element for materials with other structural levels (macro-, meso-, and micro-) within the framework of structural mechanics of materials).

The condition (14) or (15) determines also the sufficiently wide frame of mechanical fields, including fields under action of quite high frequency in dynamical problems and under quite short-wave modes of stability loss.

Finally, note once more that the abovestated analysis is approximate and seemingly has substantially the qualitative character. Nevertheless, it is sufficiently expedient, because the problem of validity ranges of continuum mechanics in analysis of mechanical fields in the modern structurally inhomogeneous materials has a character of traditionally constantly discussed problem.

So, the above-considered aspect of mechanics of nanocomposite materials allows to elaborate the constructive tool for separation of objects of nanomechanics from the general set of objects, which includes the micro-, meso-, and macroobjects too. This aspect can, like aspect 1, be related to those ones which show the distinction between mechanics of nanocomposite materials and mechanics of composite materials of the higher structural levels.

8. Aspect 7: Approaches "Bottom-Up" and "Top-Down"

The view on mechanics of nanocomposite materials in the light of approaches "bottom-up" and "top-down" seems very meaningful, since it highlights the specificity of nanolevel composite materials.

In technology, the two approaches "bottom-up" and "top-down" are generally known. Sometimes, "bottom-up" is commented as "nucleation and growth," and "top-down" is commented as "comminution and dispersion" [68].

The approach "bottom-up" consists in the making of materials, starting with the smallest particles up to more massive formations. In this approach, the most essential is the basis: the aggregate of smallest particles and their character. The basis forms the foundation for constructing the more massive volumes of material. This basis is called the bottom.

The approach "top-down" consists in the making of materials, starting with the large volumes of material (bulk materials, source of raw materials) in direction towords the smaller formations (pieces) of material. The rough material is pressed, cut, found, or in some different way formed into pieces or products. In this approach, the most important are the tool resources, by which the lower limit in sizes of product or material piece is determined.

But mechanics as one of the oldest sciences has also the "canonical" terminology; thus, the situation needs some discussion. In mechanics as science, the basic approach can be apparently meant as constructing the models of phenomena, processes, and materials. With allowance for the historical experience, the models in mechanics of materials are developed in direction of studying the structure of material with more and more fine scale of internal structure.

When the terminology above is being considered, it seems expedient to refer to the review in [69], which is published in 2005 and entitled "Nanocomposites in context (review)." This is consonant with the well-known review "Composites in context" [70], published in 1985. Let us cite for illustration one sentence from [69]:

Scientists and engineers working with fiber-reinforced composites have practiced this bottom-up approach in processing and manufacturing for decades. When designing a composite the material properties are tailored for the desired performance across various length scales. From selection and processing of matrix and fiber materials, and design and optimization of the fiber/matrix interface/interphase at the sub-micron scale to the manipulation of yarn bundles in 2-D and 3-D textiles to the lay-up of laminae in laminated composites and finally the net-shape forming of the macroscopic composite part,

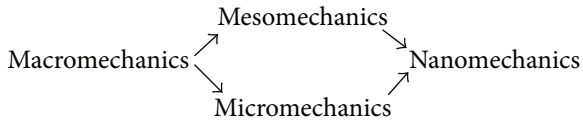

Figure 6

the integrated approach used in composites processing is a remarkable example in the successful use of the "bottom-up" approach.

This sentence testifies that the term "bottom-up" is used in technology and it was used in the making of the microcomposites (they correspond to microlevel and are studied in micromechanics).

Let us separate three moments.

Moment 1. When the nanocomposites are being made (taking into account the used, in technology, terminology), the following chain (sequence) in formation of material is realized "*aggregate of atoms (bottom) → nanomolecules, nanotubes → nanoformations (nanoparticles, nanoplates; nanowires, nanobundles, nanoropes → nanofibers) → nanocomposite*."

Thus, in technology of making the nanocomposites, the "bottom-up" approach is realized by making the material starting with the aggregate of atoms. This terminology is found everywhere in publications on nanotechnology and nanomaterials. So, in the book [70], in the approaches "bottom-up" and "top-down" subsection 1.9 is devoted. Note also that the term "bottom" was used in the Feynman famous lecture in [71].

Moment 2. In structural mechanics of materials, the basic approach consists in constructing the chain of models in direction of taking into account the more and more fine internal structure of materials. This sequential chain can be sketched out in Figure 6.

Thus, it can be thought that the terms *bottom-up approaches* and *descending approaches* have some interpretation in the structural mechanics of materials. So, the term *bottom-up approaches* corresponds to motion from the left to the right end of the level scale from the chain above. The term *descending approaches* corresponds to motion from the right to the left end of the level scale from the chain above. Let us remember that the right end corresponds to approaches, where taking into account the atom structure is obligatory.

Moment 3. Despite some distinction of terminology in technology and structural mechanics of materials, investigations on mechanics of nanocomposites are carried out within the framework of nanolevel. Therefore, at the first stage, they are carried out taking into account the atom structure under different ways of its description.

In correspondence [1, 2, 5, 62], it is proposed in mechanics of nanocomposites to apply the approaches and methods of structural macro-, meso-, and micromechanics of materials, in which the matrix and fillers are described within the framework of continuum representation. In this regard, the approaches and methods of micromechanics of materials are meant to be preferable because they are the closest in the hierarchy of structural components.

Thus, the aspect in hand is useful for mechanics of nanocomposite materials, because it allows to segregate this part of structural mechanics of material among other parts.

9. Aspect 8: Basic Approaches in Mechanics of Nanocomposite Materials

The challenging nanocomposites can be defined as the produced, at present and in the future, materials that can be applied in structural elements with allowance for features of loading and optimal correspondence of functioning of the elements under this loading.

Such optimality is realized by means of creating the anisotropy of deformation and strength properties of structural elements. The possibility of this creation is one of the most characteristic features of composites along with the high strength-to-weight ratio and high modularity.

These special properties can be formed in nanocomposites only by the straightening in directions of prevailing reinforcing the quite elongated and straightline nanoformations (CNT, nanoropes, nanofibers, and so on) as fillers, which should be coordinated with the force fluxes and be high-modulus ones.

Like the cases of macro- and microcomposites, *forecasting* the behavior of nanocomposites under mechanical actions can be realized mainly *thanks to the theoretical studies*. This is why significance of such studies is difficult to overestimate. Especially, for producing, in the future, nanocomposites, we have to take into account the strategy of technology.

It is worthy to note that at present the overwhelming number of publications on nanocomposites is devoted to analysis of nanocomposites under dispersive distribution in matrix of the comparatively short nanoformations as fillers. At that, the clearly expressed directions of reinforcing are absent. These dispersive nanocomposites can be classified as the type of hardened matrix, which is frequently reflected in terminology of publications.

But this type of engineering cannot define the progress of perspective nanocomposites, in which reinforcing is coordinated with loading.

The considerations above testify that in constructing the foundations of mechanics of nanocomposites with polymeric matrix the quite substantiated is the basic approach, which can be meant as "*set of concepts, models and statements of problems, development of methods of analysis, and obtaining the new results, which are adequate to phenomena of interest in perspective nanocomposite materials under mechanical actions*."

The formulated basic approach consists of the following four parts.

(i) Part I. Modeling of the nanoformations by the linear elastic isotropic homogeneous body with averaged values of elastic constants, which are obtained with attracting the concept of *continualization* from results

taking into account the action of forces of interatomic interaction.

(ii) Part II. Modeling of the polymeric matrix (binder) by the linear isotropic homogeneous elastic or viscoelasticbody. The similar modeling was used traditionally in constructing the foundations of mechanics of microcomposites. Under moderate temperatures or under comparatively short-time loading, a polymeric matrix in nanocomposites can be modeled by the linear isotropic elastic body.

(iii) Part III. Modeling of the interaction of nanoformations and polymeric matrix (in the thin intermediate layer with allowance for forces of interatomic interaction) by certain boundary conditions with transferring these conditions on the *geometric interface*, using the boundary conditions of *perfect contact* (continuity of stress and displacement vectors) and boundary conditions of *sliding contact for bilateral estimates* of quantities under consideration.

(iv) Part IV. Determination of the averaged values of elastic constants for nanocomposites using various methods of *homogenization*, which provides the transition to mechanics of structural members from nanocomposites.

In this way, within the framework of the basic approach, the different problems of statics, dynamics, stability, and fracture of nanocomposite materials and structural elements made of these materials are carried out.

It was mentioned before, in analysis of problems of mechanics of nanocomposites, that the model of piece-wise homogeneous medium (after realization of the concept of *continualization* for nanofillers) and the model of homogeneous anisotropic body with averaged elastic constants (after realization of the concept of *continualization* for nanofillers and the following realization of the concept of *homogenization* for the obtained piece-wise homogeneous medium) are used.

In analysis of problems in mechanics of structural elements made of nanocomposites, the application of the *model of anisotropic homogeneous body* with averaged values of elastic constants seems to be preferable.

Of course, in this part of mechanics, an analysis of multilayered constructions (e.g., constructing the models and theories of multilayered rods, plates, and shells) is actual. In this case, for each single element of construction (for each layer), the model of anisotropic homogeneous body with averaged elastic constants is used.

Within the framework of the basic approach, a row of new results is obtained.

It is necessary to point out that actually a number of reviews on different problems of mechanics of nanocomposites are published [1, 2, 5, 62, 69, 72–77].

Note also that the essential moment in the basic approach is *the second position of part III*, in concordance with which the bilateral estimates for quantities of interest are expedient to have. They are based on study of boundary conditions of perfect contact and sliding contact on *the geometrical* interface "filler-binder." The obtained, in such a way, *bilateral estimates* enable to determine values of quantities of interest for almost all various physical-chemical processes occurring in the intermediate layer between the filler and the polymeric matrix.

10. Aspect 9: Transition from Mechanics of Nanomaterials to Mechanics of Nanostructural Members

The abovestated considerations on mechanics of nanocomposites form the theoretical prerequisites for studying the basic problems arising in this part of mechanics: statical and dynamical problems, problems of stability, and fracture mechanics problems. In such studies, the statements of problems and methods of solving analogous to the approaches that are developed in mechanics of microcomposite can be used (see, e.g., multivolume editions [9–16, 23–49, 77]). In these studies, the model of piece-wise homogeneous medium and the model of homogeneous medium with averaged properties can be traditionally used.

In the studies within the framework of mechanics of structural members, it seems mostly promising and may be solely possible to apply the approach when the nanocomposite (piece-wise material) is changed on the homogeneous material with averaged properties.

Thus, in problems of mechanics of structural members made of nanocomposites, first *the principle of homogenization* is expedient to use and then to consider the nanocomposite as the homogeneous material with averaged properties.

When applied to determination of averaged properties of nanocomposites, two approaches can be seemingly singled out as follows:

Approach 1: determination of averaged constants within the framework of the model of anisotropic homogeneous body (the structural model of the first order),

Approach 2: determination of averaged parameters within the framework of the structural models of the second order.

As applied to nanocomposites, when the averaged constants are being determined within the framework of the model of anisotropic elastic homogeneous body, the statements of problems and methods of studying that are developed for granular, fibrous, and layered microcomposites of determined and stochastic structure can be applied, as they. These statements and methods are expounded in numerous publications (e.g., in [9–20]).

It is necessary to note that in this case the values of averaged constants are asymptotically exact and follow from the rigorous results obtained within the framework of three-dimensional theory under some conditions.

When applied to theory of wave propagation, these conditions correspond to the situation, when the ratios of geometrical parameter characterizing the internal structure of nanocomposite to the wavelength are tending to zero, that is, as if corresponding to the long-wave approximation.

Similar conditions are applied in other problems of mechanics of nanocomposite materials.

Thus, this aspect can be related to arguments about similarity of all four parts of structural mechanics of materials, because at present all known ways of transition from mechanics of materials to mechanics of structural members in these parts are identical.

11. Final Remarks

Thus, the considered aspects of mechanics of nanocomposite materials and structural members permit to outline the similarities and distinctions of this part of structural mechanics when comparing with the other three parts—macro-, meso-, and micromechanics of materials and structural members.

The irony of fate for mechanics of nanocomposite materials and structural members consists in that similarities are essentially more studied, and they determine the tight link among all of the four parts, which is little known beyond the mechanics of materials and structural members.

Sometimes, the nature of human perception is that distinctions are fixed more often and with significantly less impediments.

Therefore, the nanomechanics in whole is represented up to this time through the prism of distinctions despite the presence of a big corpus of similarities.

References

[1] A. N. Guz, J. J. Rushchitsky, and I. A. Guz, *Introduction to Mechanics of Nanocomposites*, Akademperiodika, Kiev, Ukraine, 2010 (Russian).

[2] A. N. Guz, A. A. Rodger, and I. A. Guz, "Developing a compressive failure theory for nanocomposites," *International Applied Mechanics*, vol. 41, no. 3, pp. 233–255, 2005.

[3] I. A. Guz, J. J. Rushchitsky, and A. N. Guz, "Mechanical models in nanomaterials," in *Handbook of Nanophysics. Principles and Methods*, K. D. Sattler, Ed., vol. 1, chapter 24, pp. 24.1–24.18, Taylor and Francis Publisher (CRC Press), Boca Raton, Fla, USA, 2010.

[4] A. N. Guz and Y. Y. Rushchitskii, "Nanomaterials: on the mechanics of nanomaterials," *International Applied Mechanics*, vol. 39, no. 11, pp. 1271–1293, 2003.

[5] I. A. Guz, A. A. Rodger, A. N. Guz, and J. J. Rushchitsky, "Developing the mechanical models for nanomaterials," *Composites A*, vol. 38, no. 4, pp. 1234–1250, 2007.

[6] C. Truesdell, *A First Course in Rational Continuum Mechanics*, The John Hopkins University, Baltimore, Md, USA, 1972.

[7] M. Born and K. Huang, *Dynamical Theory of Crystal Lattices*, Oxford University Press, Oxford, UK, 2007.

[8] L. I. Slepyan, *Mechanics of Cracks*, Sudostroenie, Leningrad, Russia, 1990 (Russian).

[9] V. T. Golovchan, Ed., *Statics ofMaterials*, vol. 1 of *Mechanics of Composites*, Naukova Dumka, Kiev, Ukraine, 1993 (Russian).

[10] N. A. Shul'ga, Ed., *Dynamics and Stability of Materials*, vol. 2 of *Mechanics of Composites*, Naukova Dumka, Kiev, Ukraine, 1993 (Russian).

[11] L. P. Khoroshun, Ed., *Statistical Mechanics and Effective Properties of Materials*, vol. 3 of *Mechanics of Composites*, Naukova Dumka, Kiev, Ukraine, 1993 (Russian).

[12] A. N. Guz and S. D. Akbarov, Eds., *Mechanics of Materials with Curved Structures*, vol. 4 of *Mechanics of Composites*, Naukova Dumka, Kiev, Ukraine, 1995 (Russian).

[13] A. A. Kaminskii, Ed., *Fracture Mechanics*, vol. 5 of *Mechanics of Composites*, Naukova Dumka, Kiev, Ukraine, 1996 (Russian).

[14] N. A. Shul'ga and V. T. Tomashevsk, Eds., *Process-Induced Stresses and Strains in Materials*, vol. 6 of *Mechanics of Composites*, Naukova Dumka, Kiev, Ukraine, 1997 (Russian).

[15] A. N. Guz, A. S. Kosmodamianskii, and V. P. Shevchenko, Eds., *Stress Concentration*, vol. 7 of *Mechanics of Composites*, Naukova Dumka, Kiev, Ukraine, 1998 (Russian).

[16] Ya. M. Grigorenko, Ed., *Statics of Structural Members*, vol. 8 of *Mechanics of Composites*, Naukova Dumka, Kiev, Ukraine, 1999 (Russian).

[17] V. D. Kubenko, Ed., *Dynamics of Structural Members*, vol. 9 of *Mechanics of Composites*, Naukova Dumka, Kiev, Ukraine, 1999 (Russian).

[18] I. Yu. Babich, Ed., *Stability of Structural Members*, vol. 10 of *Mechanics of Composites*, Naukova Dumka, Kiev, Ukraine, 2001 (Russian).

[19] Ya. M. Grigorenko and Yu. N. Shevchenko, Eds., *Numerical Methods*, vol. 11 of *Mechanics of Composites*, Naukova Dumka, Kiev, Ukraine, 2002 (Russian).

[20] A. N. Guz and L. P. Khoroshun, Eds., *Applied Investigations*, vol. 12 of *Mechanics of Composites*, Naukova Dumka, Kiev, Ukraine, 2003 (Russian).

[21] A. N. Guz, "Three-dimensional theory of stability of a carbon nanotube in a matrix," *International Applied Mechanics*, vol. 42, no. 1, pp. 19–31, 2006.

[22] I. A. Guz, A. A. Rodger, A. N. Guz, and J. J. Rushchitsky, "Predicting the properties of micro- and nanocomposites: from the microwhiskers to the bristled nano-centipedes," *Philosophical Transactions of the Royal Society A*, vol. 366, no. 1871, pp. 1827–1833, 2008.

[23] A. G. Metcalfe, Ed., *Interfaces in Metal Matrix Composites*, vol. 1 of *Composite Materials*, Academic Press, New York, NY, USA, 1974.

[24] G. P. Sendeckyi, Ed., *Mechanics of Composite Matreials*, vol. 2 of *Composite Materials*, Academic Press, New York, NY, USA, 1974.

[25] B. Noton, Ed., *Application of Composite Materials in Technics*, vol. 3 of *Composite Materials*, Academic Press, New York, NY, USA, 1974.

[26] B. Krider, Ed., *Composite Materials with Metallic Matrix*, vol. 4 of *Composite Materials*, Academic Press, New York, NY, USA, 1974.

[27] L. J. Broutman, Ed., *Fracture and Fatigue*, vol. 5 of *Composite Materials*, Academic Press, New York, NY, USA, 1974.

[28] E. P. Plueddemann, Ed., *Interfaces in Polymer Matrix Composites*, vol. 6 of *Composite Materials*, Academic Press, New York, NY, USA, 1974.

[29] C. C. Chamis, Ed., *Structural Design and Analysis—Part 1*, vol. 7 of *Composite Materials*, Academic Press, New York, NY, USA, 1975.

[30] C. C. Chamis, Ed., *Structural Design and Analysis—Part 2*, vol. 7 of *Composite Materials*, Academic Press, New York, NY, USA, 1975.

[31] T.-W. Chou, Ed., *Fiber Reinforcements and General Theory of Composites*, vol. 1 of *Comprehensive Composite Material*, Elsevier, London, UK, 2006.

[32] R. Talreja and J. A. Mänson, Eds., *Polymer Matrix Composites*, vol. 2 of *Comprehensive Composite Material*, Elsevier, London, UK, 2006.

[33] T. W. Clyne, Ed., *Metal Matrix Composites*, vol. 3 of *Comprehensive Composite Material*, Elsevier, London, UK, 2006.

[34] R. Warren, Ed., *Carbon/Carbon, Cement and Ceramic Composites*, vol. 4 of *Comprehensive Composite Material*, Elsevier, London, UK, 2006.

[35] L. Carlsson, R. L. Crane, and K. Uchino, Eds., *Test Methods, Nondestructive Evaluation, and Smart Materials*, vol. 5 of *Comprehensive Composite Material*, Elsevier, London, UK, 2006.

[36] W. G. Bader, K. Kedsvard, and Y. Sawada, Eds., *Design and Applications*, vol. 6 of *Comprehensive Composite Material*, Elsevier, London, UK, 2006.

[37] I. Milne, R. O. Ritchie, and B. Karihaloo, Eds., *Structural Integrity Assessment—Examples and Case Studies*, vol. 1 of *Comprehensive Structural Integrity*, Elsevier, London, UK, 2006.

[38] B. Karihaloo and W. G. Knauss, Eds., *Fundamental Theories and Mechanisms of Failure*, vol. 2 of *Comprehensive Structural Integrity*, Elsevier, London, UK, 2006.

[39] R. de Borst and H. A. Mang, Eds., *Numerical and Computational Methods*, vol. 3 of *Comprehensive Structural Integrity*, Elsevier, London, UK, 2006.

[40] R. O. Ritchie and Y. Murakami, Eds., *Cyclic Loading and Fatigue*, vol. 4 of *Comprehensive Structural Integrity*, Elsevier, London, UK, 2006.

[41] A. Saxena, Ed., *Creep and High-Temperature Failure*, vol. 5 of *Comprehensive Structural Integrity*, Elsevier, London, UK, 2006.

[42] J. Petit and P. Scott, Eds., *Environmentally Assisted Fracture*, vol. 6 of *Comprehensive Structural Integrity*, Elsevier, London, UK, 2006.

[43] R. A. Ainsworth and K.-H. Schwalbe, Eds., *Practical Failure Assessment Methods*, vol. 7 of *Comprehensive Structural Integrity*, Elsevier, London, UK, 2006.

[44] W. Gerberich and W. Yang, Eds., *Interfacial and Nanoscale Failure*, vol. 8 of *Comprehensive Structural Integrity*, Elsevier, London, UK, 2006.

[45] Y.-W. Mai and S.-H. Teoh, Eds., *Bioengineering*, vol. 9 of *Comprehensive Structural Integrity*, Elsevier, London, UK, 2006.

[46] *Indexes*, vol. 10 of *Comprehensive Structural Integrity*, Elsevier, London, UK, 2006.

[47] L. P. Khoroshun, Ed., *Mechanics of Materials*, vol. 1 of *Mechanics of Composite Materials and Structural Members*, Naukova Dumka, Kiev, Ukraine, 1982 (Russian).

[48] Ya. M. Grigorenko, Ed., *Mechanics of Structural Members*, vol. 2 of *Mechanics of Composite Materials and Structural Members*, Naukova Dumka, Kiev, Ukraine, 1982 (Russian).

[49] *Applied Investigations*, vol. 3 of *Mechanics of Composite Materials and Structural Members*, Naukova Dumka, Kiev, Ukraine, 1983 (Russian).

[50] C. Cattani and J. J. Rushchitsky, *Wavelet and Wave Analysis as Applied to Materials with Micro or Nanostructures*, World Scientific Publishing, Singapore, 2007.

[51] Y. Y. Rushchitskii, "Extension of the microstructural theory of two-phase mixtures to composite materials," *International Applied Mechanics*, vol. 36, no. 5, pp. 586–614, 2000.

[52] J. J. Rushchitsky and S. I. Tsurpal, *Waves in Materials with Microstructure*, SP Timoshenko Institute of Mechanics, Kiev, Ukraine, 1998 (Russian).

[53] A. Bedford, G. S. Drumheller, and H. J. Sutherland, "On modeling the dynamics of composite materials," in *Mechanics Today*, S. Nemat-Nasser, Ed., vol. 3, pp. 1–54, Pergamon Press, New York, NY, USA, 1976.

[54] H. S. Katz and J. V. Milewski, Eds., *Handbook of Fillers and Reinforcements for Plastics*, Van Nostrand Reinhold Company, New York, NY, USA, 1978.

[55] M. A. Biot, "Surface instability in finite anisotropic elasticity under initial stress," *Proceedings of the Royal Society A*, vol. 273, no. 1354, pp. 329–339, 1963.

[56] A. N. Guz, *Fundamentals of Three-Dimensional Theory of Stability of Deforming Bodies*, Vyshcha Shkola, Kiev, Ukraine, 1986 (Russian).

[57] A. N. Guz, *Fundamentals of Three-Dimensional Theory of Stability of Deformable Bodies*, Springer, Berlin, Germany, 1999.

[58] A. N. Guz, Ed., *Fracture in Structure of Material*, vol. 1 of *Fundamentals of Fracture Mechanics of Composites under Compression*, Litera, Kiev, Ukraine, 2008 (Russian).

[59] A. N. Guz, Ed., *Related Mechanisms of Fracture*, vol. 2 of *Fundamentals of Fracture Mechanics of Composites under Compression*, Litera, Kiev, Ukraine, 2008 (Russian).

[60] M. A. Biot, "Fundamental skin effect in anisotropic solid mechanics," *International Journal of Solids and Structures*, vol. 2, no. 4, pp. 645–663, 1966.

[61] N. A. Shul'ga, *Foundations of Mechanics of Layered Media of Periodic Structure*, Naukova Dumka, Kiev, Ukraine, 1981 (Russian).

[62] A. N. Guz, J. J. Rushchitsky, and I. A. Guz, "Establishing fundamentals of the mechanics of nanocomposites," *International Applied Mechanics*, vol. 43, no. 3, pp. 247–271, 2007.

[63] S. C. Tjong, *Carbon Nanotube Reinforced Composites: Metal and Ceramic Matrices*, Wiley-VCH, Weinheim, Germany, 2009.

[64] D. W. Brenner, "Empirical potential for hydrocarbons for use in simulating the chemical vapor deposition of diamond films," *Physical Review B*, vol. 42, no. 15, pp. 9458–9471, 1990.

[65] J. Tersoff, "Empirical interatomic potential for carbon, with applications to amorphous carbon," *Physical Review Letters*, vol. 61, no. 25, pp. 2879–2882, 1988.

[66] J. Tersoff, "New empirical approach for the structure and energy of covalent systems," *Physical Review B*, vol. 37, no. 12, pp. 6991–7000, 1988.

[67] E. Hernández, C. Goze, P. Bernier, and A. Rubio, "Elastic properties of single-wall nanotubes," *Applied Physics A*, vol. 68, no. 3, pp. 287–292, 1999.

[68] J. Ramsden, *Nanotechnology*, Ventus Publishing ApS, Copenhagen, Denmark, 2010.

[69] E. T. Thostenson, C. Li, and T.-W. Chou, "Nanocomposites in context," *Composites Science and Technology*, vol. 65, no. 3-4, pp. 491–516, 2005.

[70] A. Kelly, "Composites in context," *Composites Science and Technology*, vol. 23, no. 3, pp. 171–199, 1985.

[71] N. Wilson, K. Kannangara, G. Smith, M. Simmons, and B. Raguse, *Nanotechnology: Basic Science and Emerging Technologies*, Chapman and Hall/CRC, Boca Raton, Fla, USA, 2002.

[72] V. A. Buryachenko, A. Roy, K. Lafdi, K. L. Anderson, and S. Chellapilla, "Multi-scale mechanics of nanocomposites including interface: experimental and numerical investigation," *Composites Science and Technology*, vol. 65, no. 15-16, pp. 2435–2465, 2005.

[73] A. A. Guz, J. J. Rushchitsky, and I. A. Guz, "Comparative computer modeling of carbon-polymer composites with carbon or graphite microfibers or carbon nanotubes," *Computer Modeling in Engineering and Sciences*, vol. 26, no. 3, pp. 139–156, 2008.

[74] A. K.-T. Lau and D. Hui, "The revolutionary creation of new advanced materials—carbon nanotube composites," *Composites B*, vol. 33, no. 4, pp. 263–277, 2002.

[75] H. S. Nalwa, *Handbook of Nanostructured Materials and Nanotechnology*, vol. 3, Academic Press, San Diego, Calif, USA, 2000.

[76] D. Srivastava, C. Wei, and K. Cho, "Nanomechanics of carbon nanotubes and composites," *Applied Mechanics Reviews*, vol. 56, no. 2, pp. 215–229, 2003.

[77] Y.-W. Mai and Z. Yu, Eds., *Polymer Nanocomposites*, Woodhead Publishing Limited, Cambridge, UK, 2009.

Hindawi Publishing Corporation
Journal of Nanotechnology
Volume 2013, Article ID 138457, 10 pages
http://dx.doi.org/10.1155/2013/138457

Research Article

LDPE/HDPE/Clay Nanocomposites: Effects of Compatibilizer on the Structure and Dielectric Response

B. Zazoum, E. David, and A. D. Ngô

Département de Génie Mécanique, École de Technologie Supérieure (ETS), 1100 Notre-Dame Ouest, Montréal, QC, Canada H3C 1K3

Correspondence should be addressed to B. Zazoum; bouchaib.zazoum.1@ens.etsmtl.ca

Received 26 July 2013; Accepted 16 August 2013

Academic Editor: John Zhanhu Guo

PE/clay nanocomposites were prepared by mixing a commercially available premixed polyethylene/O-MMT masterbatch into a polyethylene blend matrix containing 80 wt% low-density polyethylene and 20 wt% high-density polyethylene with and without anhydride modified polyethylene (PE-MA) as the compatibilizer using a corotating twin-screw extruder. In this study, the effect of nanoclay and compatibilizer on the structure and dielectric response of PE/clay nanocomposites has been investigated. The microstructure of PE/clay nanocomposites was characterized using wide-angle X-ray diffraction (WAXD) and a scanning electron microscope (SEM). Thermal properties were examined using differential scanning calorimetry (DSC). The dielectric response of neat PE was compared with that of PE/clay nanocomposite with and without the compatibilizer. The XRD and SEM results showed that the PE/O-MMT nanocomposite with the PE-MA compatibilizer was better dispersed. In the nanocomposite materials, two relaxation modes are detected in the dielectric losses. The first relaxation is due to a Maxwell-Wagner-Sillars interfacial polarization, and the second relaxation can be related to dipolar polarization. A relationship between the degree of dispersion and the relaxation rate f_{max} of Maxwell-Wagner-Sillars was found and discussed.

1. Introduction

There has been growing interest in polymer/nanoclay nanocomposites in recent years because of their outstanding properties at low loading levels as compared with conventional composites. It has been observed that adding small quantities of nanoclay to some thermoplastics as a reinforcing filler to form nanocomposite materials has not only led to more improved mechanical and thermal properties, but also to an enhancement of the dielectric strength and partial discharge resistance [1–10]. However, the understanding of the role of the interfaces of the nanofillers with the molecular mobility mechanism is still rather unsatisfactory.

Although there are different processing methods for preparing nanocomposites, the most widely used technique is the melt-compounding method using a twin-screw extruder, because this technique features economic benefits and ecological advantages. The main challenge in the fabrication of nanocomposites is dispersion of the individual clay platelets into the polymer matrix, due to the incompatibility of hydrophobic matrix with hydrophilic nanoclay [11]. Rendering clay platelets more hydrophobic requires a surface treatment, which is accomplished via ion-exchange reactions with cationic surfactants using quaternary alkyl ammonium cations [12]. For more polar polymers, such as nylon, a surface treatment of layered silicate with an alkyl-ammonium surfactant is sufficient to facilitate exfoliation of the nanofiller within the polymer matrix in some process conditions. However, in the case of polyethylene, it is necessary to use maleic anhydride modified polyethylene PE-g-MA as a compatibilizer to facilitate exfoliation. There are two parameters that contribute to achieving the exfoliation of layered silicates: (1) maleic anhydride content and (2) molecular weight. In general, maleic anhydride modified polyethylene PE-g-MA possesses these two required factors and is widely used as compatibilizer for preparing polyethylene/clay nanocomposites. The most commonly used techniques for evaluating the quality of the dispersion of the nanoclay within the polymer matrix are scanning electron microscopy (SEM), transmission electron microscopy (TEM), and X-ray diffraction (XRD). Only few publications in this field report the use of dielectric methods, which are able to characterize

the level of dispersion and can be combined with microscopic measurements [13–17].

Polyethylene is one of the polyolefins that is used most extensively as ground-wall insulation for medium- to high-voltage applications, and especially for cable insulation, due to its desirable electrical insulating properties, including low relative permittivity ε', low dielectric loss ε'', and high dielectric breakdown strength.

Only a few works have focused on the structure/dielectric response relationship of polyethylene blend nanocomposites. The main objective of this paper is to examine the effect of nanoclay and compatibilizers on the structure and dielectric response of PE/clay nanocomposites prepared by melt-compounding using a corotating twin-screw extruder,and to understand the relationship between these two properties.

2. Experiment

2.1. Materials. The matrix consisted of low-density polyethylene (LDPE, LF-Y819-A, NOVA Chemicals) with a melt flow index (MFI) of 0.75 g/10 min and a density of 0.919 g/cm^3 and high-density polyethylene (HDPE, DGDP-6097 NT 7, DOW) with a melt flow index (MFI) of 10.5 g/10 min and a density of 0.948 g/cm^3. The compatibilizer was anhydride modified polyethylene (PE-MA, E226, Dupont) with a melt flow index (MFI) of 1.75 g/10 min and a density of 0.930 g/cm^3. A commercially available masterbatch of LLDPE/O-MMT (NanoMax) containing 50% organomodified montmorillonite (OMMT) was supplied by Nanocor.

2.2. Preparation of Nanocomposites. The blend of LDPE/HDPE was fixed at a weight ratio of 80/20. The LDPE, HDPE, PEMA, and the commercial masterbatch of LLDPE/O-MMT were dried at 40°C in a vacuum oven for a minimum of 48 hrs prior to extrusion. Nanocomposites were prepared by an extrusion process using a corotating twin-screw extruder (Haake Polylab Rheomex OS PTW16, $D = 16$ mm, $L/D = 40$) coupled with a Haake Metering Feeder to control the feed rate. The temperature profile used in this study was 170–180°C from hopper to die, the feed rate was fixed at 1 kg/hr, and the screw speed was set at 140 rpm. All materials were manually premixed before introduction into the twin-screw extruder. The pellets that were obtained after extrusion were press-molded using an electrically heated hydraulic press to form thin plates (1.2 mm thick). The molding temperature and pressure were 178°C and 5 MPa, respectively. A summary of the compositions of the PE/clay nanocomposites used in this paper is collected in Table 1.

3. Characterization and Measurements

3.1. Differential Scanning Calorimetry (DSC). Thermal parameters (melting temperature, crystallization temperature, and crystallinity) of neat PE, PE/O-MMT, and PE/O-MMT/PE-MA nanocomposites were determined using a Perkin-Elmer DSC Pyris 1 instrument. The calibration of the DSC was performed using indium. All samples had the same weight (approximately 5.0 mg), and the PE and its nanocomposites were heated from 30°C to 180°C during each run at a heating rate of 10°C/min in nitrogen atmosphere. The endothermic and exothermic diagrams were recorded as a function of temperature.

3.2. X-Ray Diffraction (XRD). X-ray diffraction (XRD) was employed in order to assess the degree of dispersion and exfoliation or intercalation state of the nanoclay in the polymer matrix. XRD patterns were identified using a diffractometer (PANalytical X'Pert Pro) with Kα radiation at a wavelength λ of 1.5418 Å and operated at an accelerating voltage of 40 kV and an electrical current of 45 mA. The scanning was conducted from 2° to 9°, with a scan rate of 0.6°/min. The intercalate spacing d_{001} was calculated using Bragg's law:

$$2d \sin\theta = \lambda, \tag{1}$$

where d, θ, and λ represent the interlayer distance of the clay, the measured diffraction angle, and the wavelength, respectively.

3.3. Microscopical Observations. The morphology of the samples was examined using a Hitachi scanning electron microscope (SEM). The samples were first cut in a microtome (Ultraculeika) equipped with a glass knife and then coated with a 2 nm thick layer of platinum in order to avoid electrostatic charging during microscopic observations. The operating voltage was fixed at the lowest possible voltage (5 kV) in order to prevent polymer damage and maintain high-resolution images.

3.4. Dielectric Relaxation Spectroscopy. Dielectric relaxation spectroscopy experiments were carried out using a Novocontrol alpha-N in the 10^{-2} to 10^5 Hz frequency domain at temperatures of 30°, 40°, 50°, 60°, and 70°C. The temperature was controlled using a Novotherm system with a stability of 0.5°C.

Prior to all dielectric spectroscopy measurements, the samples measuring 40 mm in diameter and 1.20 mm in thickness were dried at 50°C in a vacuum oven for 24 hrs and then sandwiched between two gold-plated electrodes measuring 40 mm in diameter to form a parallel-plate geometry capacitor.

The complex dielectric permittivity is given by

$$\varepsilon^*(\omega) = \varepsilon'(\omega) - i\varepsilon''(\omega), \tag{2}$$

where $\varepsilon'(\omega)$ represents the real part, $\varepsilon''(\omega)$ represents the imaginary part, and $\omega = 2\pi f$ represents the angular frequency.

The experimental dielectric data can be fitted into the Havrilialk-Negami equation as shown below:

$$\varepsilon^* = \varepsilon_\infty + \sum_{i=1}^{n} \frac{\Delta\varepsilon_i}{\left(1 + (i\omega\tau_i)^{\alpha_i}\right)^{\beta_i}}, \tag{3}$$

where ε_∞ represents the high frequency permittivity, $\Delta\varepsilon_i$ represents the ith dielectric relaxation strength, τ_i represents

Table 1: Sample formulation and designation.

Sample designation	LLDPE (wt%)	LDPE/HDPE (wt%)	PE-MA (wt%)	O-MMT (wt%)
MB	50	—	—	50
PE	—	100	0	0
PE/O-MMT	5	90	0	5
PE/O-MMT/PE-MA	5	80	10	5

the relaxation time of the ith relaxation, n represents the number of relaxation processes, and α_i and β_i ($0 < \alpha \leq 1$, $\alpha\beta \leq 1$) represent the shape parameters describing symmetric and asymmetric broadening of the relaxation spectra. At low frequency, the influence of the charge carrier fluctuations must be taken into consideration. The complex permittivity can then be expressed as

$$\varepsilon^* = \varepsilon_\infty + \sum_{i=1}^{n} \left[\frac{\Delta\varepsilon_i}{\left(1 + (i\omega\tau_i)^{\alpha_i}\right)^{\beta_i}} \right] + \frac{\sigma_0}{\varepsilon_0 (i\omega)^s}. \quad (4)$$

By using (2), (3), and (4), the real part $\varepsilon'(\omega)$ and the imaginary part $\varepsilon''(\omega)$ of the complex dielectric permittivity $\varepsilon^*(\omega)$ can be written as

$$\begin{aligned}
\varepsilon'(\omega) = \varepsilon_\infty + \sum_{i=1}^{n} \Bigg[& \Delta\varepsilon_i \cos(\beta_i\varphi_i) \\
& \times \left(\left(1 + 2(\omega\tau_i)^{\alpha_i} \sin\left(\frac{\pi(1-\alpha_i)}{2} \right) + (\omega\tau)^{2\alpha_i} \right)^{\beta_i/2} \right)^{-1} \Bigg] \\
& + \frac{\sigma_o \omega^{-s}}{\varepsilon_0} \cos\left(\frac{\pi s}{2} \right), \\
\varepsilon''(\omega) = & \sum_{i=1}^{n} \left[\frac{\Delta\varepsilon_i \sin(\beta_i\varphi_i)}{\left(1 + 2(\omega\tau_i)^{\alpha_i} \sin(\pi(1-\alpha_i)/2) + (\omega\tau)^{2\alpha_i} \right)^{\beta_i/2}} \right] \\
& + \frac{\sigma_o \omega^{-s}}{\varepsilon_0} \sin\left(\frac{\pi s}{2} \right),
\end{aligned} \quad (5)$$

where

$$\varphi_i = \tan^{-1}\left[\frac{(\omega\tau_i)^{\alpha_i} \cos(\pi(1-\alpha_i)/2)}{1 + (\omega\tau_i)^{\alpha_i} \sin(\pi(1-\alpha_i)/2)} \right], \quad (6)$$

where σ_o represents dc conductivity and s represents an adjustable parameter. In the case of pure electronic dc conductivity, $s = 1$.

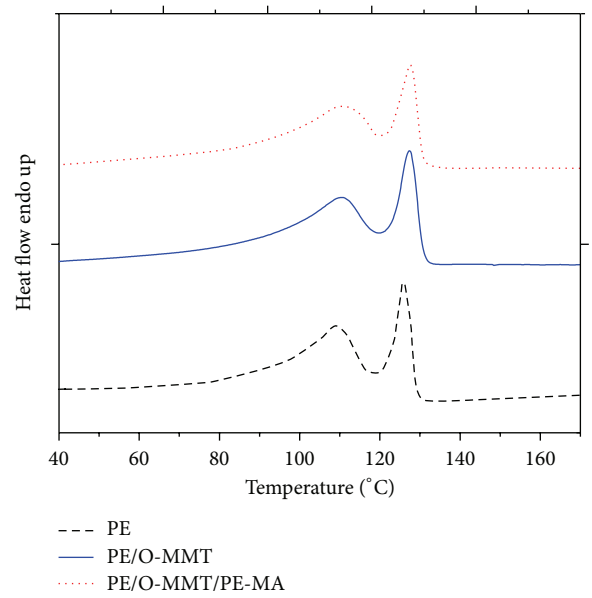

Figure 1: DSC heating thermograms of neat PE, PE/O-MMT, and PE/O-MMT/PE-MA nanocomposites.

4. Results and Discussion

4.1. Thermal Properties. Differential scanning calorimetry (DSC) was used to measure the melting temperatures, crystallization temperatures, and fusion enthalpy ΔH_F. The degree of crystallinity was calculated as expressed by the following equation:

$$\%\chi = \frac{\Delta H_F}{\Delta H_F^0 (1 - \varphi)}, \quad (7)$$

where ΔH_F represents the heat of fusion (J/g), ΔH_F^0 represents the theoretical heat of fusion of 100% crystalline PE (293 J/g), and φ represents the weight fraction of O-MMT in the composites.

The melting and crystallization curves of neat polyethylene and its nanocomposites are depicted in Figures 1 and 2, respectively. The thermal parameters derived from these curves are shown in Table 2. Differential scanning calorimetry (DSC) thermograms revealed two different peak temperatures, with the first melting temperature related to LDPE and the second melting temperature related to HDPE. The melting point peak of LLDPE was not detected due to the low concentration of LLDPE in the nanocomposites. The DSC results clearly showed that the melting temperature,

Table 2: DSC data for PE and its nanocomposites.

Sample	LDPE (T_m, °C)	HDPE (T_m, °C)	LDPE (T_c, °C)	HDPE (T_c, °C)	Heat of fusion of PE (J/g)	Crystallinity of PE (%)
PE	109.4	125.8	97.3	113.5	115.8	39.5
PE/O-MMT	110.6	127.4	97.4	113.4	114.4	41.1
PE/O-MMT/PE-MA	110.9	127.7	98.8	112.7	113.7	40.8

Table 3: 2θ and d_{001} data for the different nanocomposites.

Sample	2θ (°)	d_{001} (nm)
MB	3.13	2.82
PE/O-MMT	2.93	3.02
PE/O-MMT/PEMA	2.72	3.25

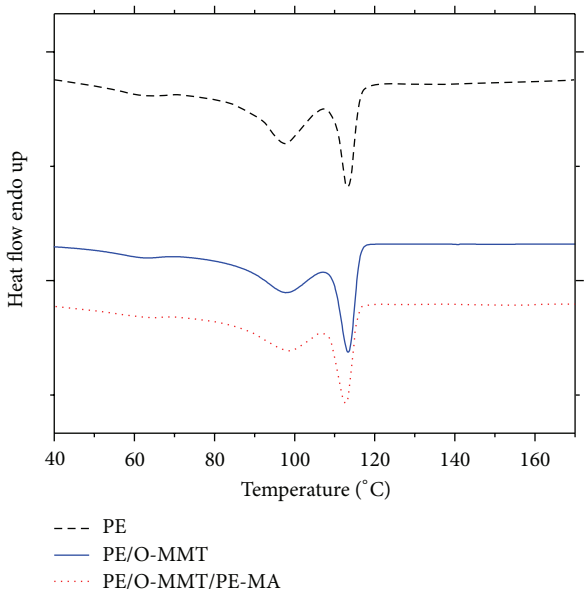

Figure 2: DSC cooling thermograms of neat PE, PE/O-MMT, and PE/O-MMT/PE-MA nanocomposites.

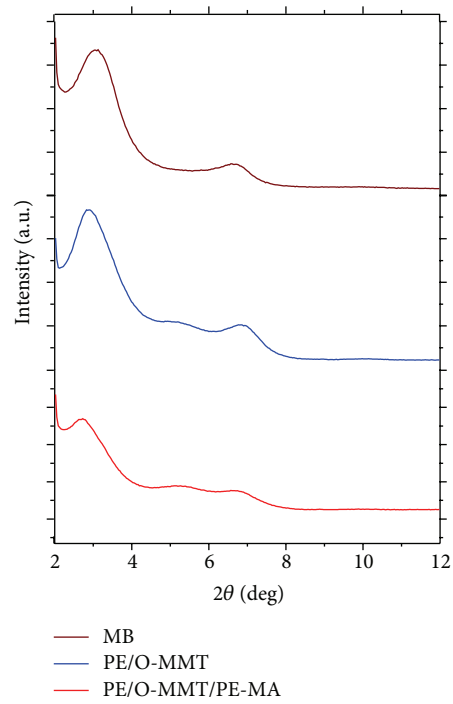

Figure 3: X-ray diffraction patterns for MB and PE nanocomposites with and without compatibilizer.

crystallization temperature, and crystallinity of PE/O-MMT and PE/O-MMT/PE-MA are almost the same as those of neat PE. This behavior suggests that the presence of the organoclay did not create a nucleating effect. The same resultants were found by Morawiec et al. [18].

4.2. Wide-Angle X-Ray Diffraction (WAXD). Figure 3 shows the X-ray diffraction spectra for the O-MMT masterbatch, PE/O-MMT, and PE/O-MMT/PE-MA nanocomposites. The diffraction peak for the O-MMT masterbatch is approximately $2\theta = 3.13^\circ$, which corresponds to a d_{001} value of 2.82 nm calculated using the Bragg law (Table 3). When the O-MMT masterbatch was diluted with pure PE to create PE/O-MMT nanocomposites, the diffraction peak was found to shift to a smaller angle of 2.93°, indicating the increase in d_{001} spacing of the galleries of the organoclay. This improvement in the dispersion was due to the processing conditions for the fabrication of nanocomposites. For the ternary nanocomposites PE/O-MMT/PE-MA, the diffraction peak was observed at a lower angle of 2.73°, corresponding to an increase in intercalate spacing d_{001} to 3.25 nm. On the other hand, the reduction in the diffraction intensity accompanied by the broadening of the basal peak in the PE/O-MMT/PE-MA nanocomposites suggests that the degree of dispersion of the nanoclay within the polymer matrix was improved and that these compatibilized nanocomposites contain a significant proportion of exfoliated nanoclay in the final nanocomposites. This is due to the polar interactions between the maleic anhydride groups in the PE-MA and the OH groups of clay which lead to a formation of a covalent bond between clay and compatibilizer and help polymer chains to penetrate the galleries of the organoclay easily [6, 19, 20]. Since PE-MA has a high molecular weight (low melt index), the shear stress was significant, which led to an increase in the delamination of the clay platelets [1, 21–27].

4.3. Morphological Characterizations by SEM. In order to confirm the XRD results, the morphology of the nanocomposites was observed using a scanning electronic microscopy

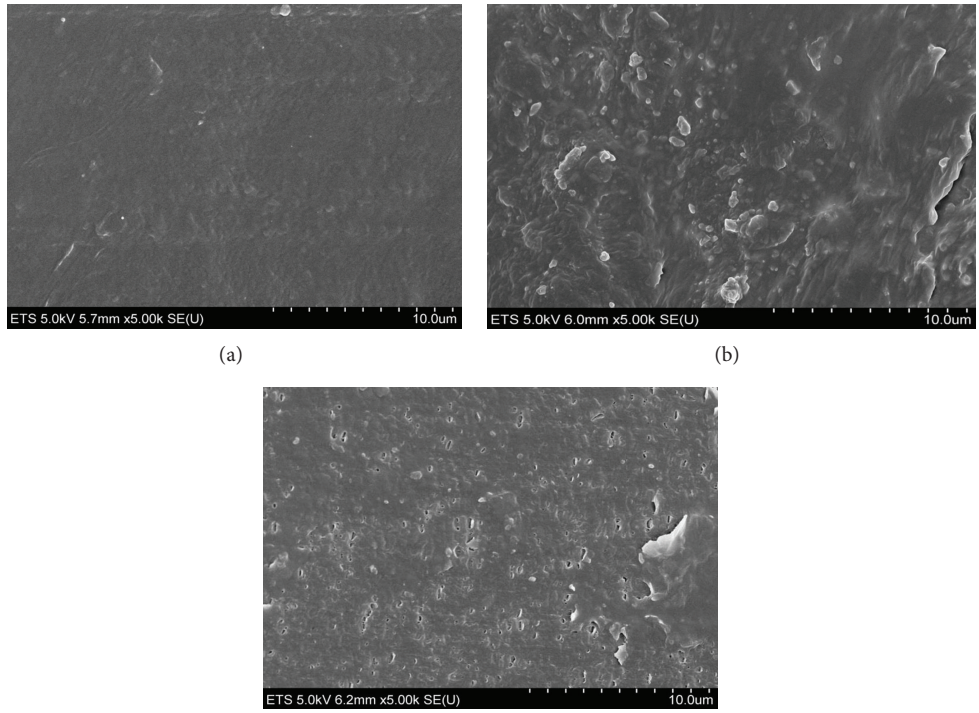

Figure 4: Representative SEM micrographs for (a) neat PE, (b) PE/O-MMT, and (c) PE/OMMT/PE-MA.

(SEM). Figure 4 shows the morphology of neat PE (Figure 4(a)), PE/O-MMT (Figure 4(b)), and the ternary nanocomposites PE/O-MMT/PE-MA (Figure 4(c)) at a magnification of 5,000. For PE/O-MMT nanocomposites, the existence of the clay aggregates or tactoids can be seen at the micrometer level, and therefore, the morphology is not homogeneous, which reveals a poor intercalated/exfoliated structure. However, when the compatibilizer was added, it was observed that the density and size of the aggregates decreased, which indicates that the dispersion of nanoclays within the polymer matrix is much better. This is consistent with the higher intercalate spacing d_{001} and the reduction in the diffraction intensity accompanied by the broadening of the peak observed in the XRD results (Figure 3 and Table 3).

4.4. Broadband Dielectric Spectroscopy. Polyethylene is classified as a nonpolar polymer with low dielectric permittivity. In general, this type of material exhibits no notable or significant ionic, interfacial, or dipolar polarization, being characterized by low flat dielectric losses. As observed from Figure 5(a), the relative permittivity (ε') of neat PE remains essentially constant in the 10^{-2} to 10^{5} frequency range, showing a small decrease when the temperature is increased. The slight decrease in (ε') at higher temperatures can be related to a combination of water evaporation and a decrease in the density [17]. However, the dielectric loss (ε'') of neat PE at low frequency (Figure 5(b)) shows a significant increase, which can be attributed to the contribution of charge carriers leading to various forms of conductivity and electrode polarization [28]. This is the so-called low-frequency dispersion. As expected, no relaxation process is detected in this material.

For PE/O-MMT nanocomposites, Figure 6 shows the frequency dependence of relative permittivity ε' and dielectric loss ε'' at various temperatures. It can be seen that the relative permittivity ε' shows two sharp decreases (Figure 6(a)), corresponding to the two peaks in the dielectric losses ε'' (Figure 6(b)). This indicates that the nanocomposites exhibited two dielectric relaxation processes. It is evident that the ε'' peaks observed in PE/OMMT nanocomposites are due to the addition of nanoclay, because no dielectric relaxations were observed for the neat PE. The peaks of the relaxation processes presented in the nanocomposites were shifted to higher frequencies as the temperature was increased. This change shows that the relaxation processes exhibited thermal activation behaviour.

In order to clearly show the relaxation processes observed in PE/O-MMT nanocomposites, the dielectric loss (ε'') was plotted as a function of the frequency and temperature in a 3D representation (Figure 7). Two relaxation modes were observed in the dielectric losses. The first relaxation was detected at low frequency, and it is attributable to a Maxwell-Wagner-Sillars polarization associated with the blocking of charges at the interfaces between two inhomogeneous phases with different conductivity, such as the polymer matrix and the silicates filler [29–31]. The second relaxation, which was detected at high frequency, can be attributed to dipolar polarization associated with the polar characteristic of the intercalant that was used for surface treatment of

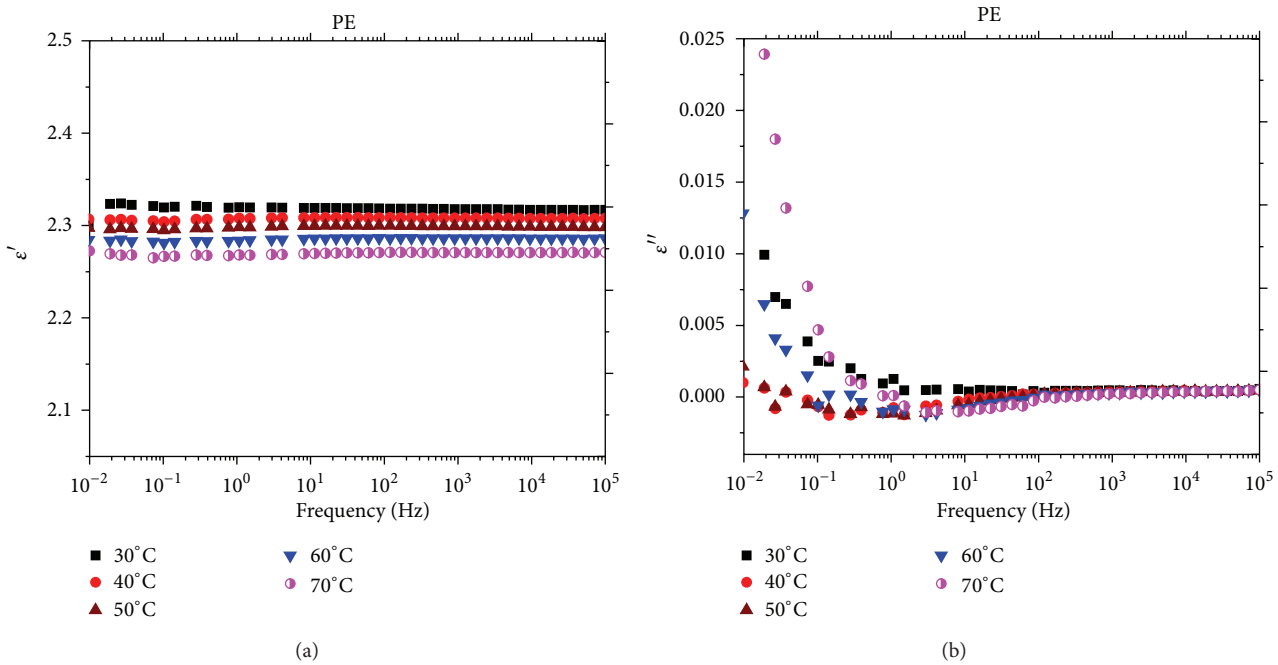

Figure 5: Relative permittivity ε' (a) and dielectric loss ε'' (b) versus frequency at various temperatures observed for the neat PE blend.

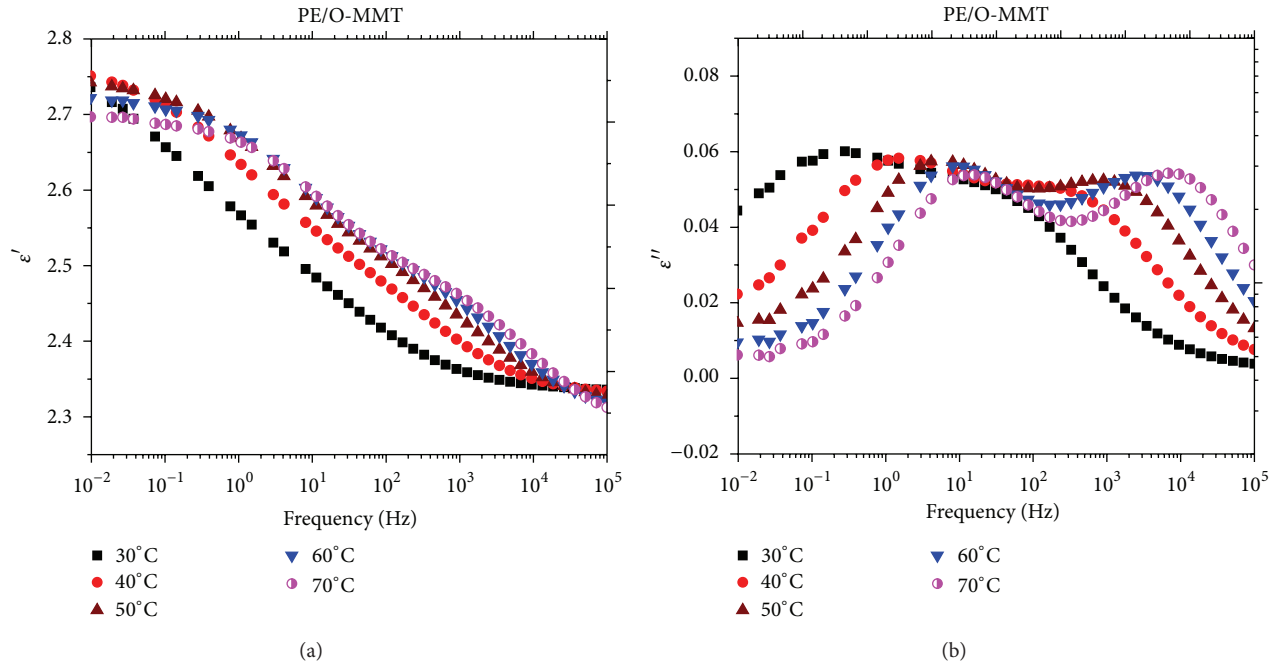

Figure 6: Relative permittivity ε' (a) and dielectric loss ε'' (b) for PE/O-MMT nanocomposites versus frequency at different temperatures.

montmorillonite clay in order to improve compatibility and dispersion of the hydrophilic clay within the hydrophobic polymer matrix.

The experimental data related to the dielectric loss ε'' for PE/O-MMT nanocomposites were fitted into the Havrilialk-Negami function (Figure 8), and the optimum dielectric parameters are shown in Table 4.

Figure 9 shows the frequency dependence of the permittivity ε' (Figure 9(a)) and the dielectric loss ε'' (Figure 9(b)) for PE/O-MMT/PE-MA. As observed for PE/O-MMT, the two relaxation processes are also presented for these compatibilized nanocomposites. It can be seen that the relaxation peaks are more thermally activated in PE/O-MMT/PE-MA than in PE/O-MMT.

In order to study the temperature dependence of both relaxation processes for the PE/O-MMT nanocomposites, the relaxation rate f_{max} of the Maxwell-Wagner-Sillars and dipolar polarization processes were plotted versus inverse

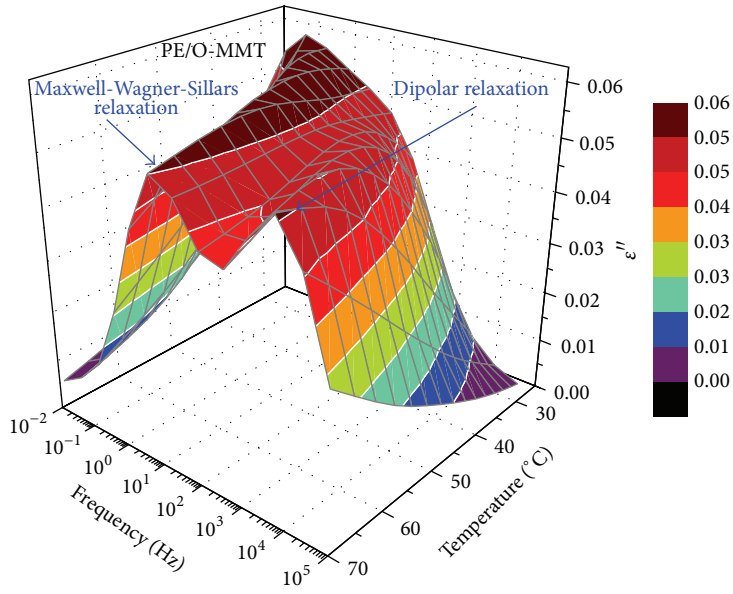

Figure 7: Dielectric loss (ε'') for PE/O-MMT nanocomposites versus frequency at various temperatures, plotted in 3D representation.

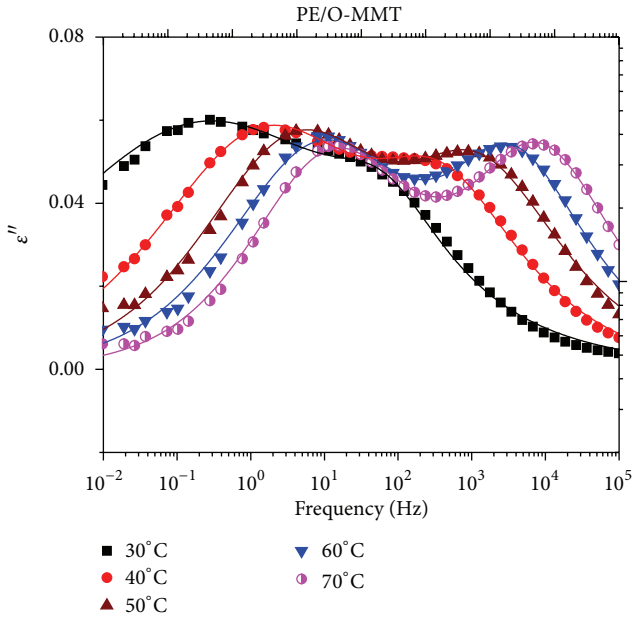

Figure 8: Dielectric loss ε'' for PE/O-MMT nanocomposites versus frequency at different temperatures with the optimum fitting curves for the Havrilialk-Negami equation.

Table 4: Optimum fit parameters for MWS and dipolar relaxations in Figure 8.

(a)

	MWS polarization			
T (°C)	α_1	β_1	$\Delta\varepsilon_1$	τ_1 (s)
30	0.29	1.00	0.50	0.56
40	0.43	1.00	0.32	0.11
50	0.48	1.00	0.27	0.04
60	0.49	0.98	0.26	0.02
70	0.55	0.89	0.23	0.01

(b)

	Dipolar polarization			
T (°C)	α_2	β_2	$\Delta\varepsilon_2$	τ_2 (s)
30	0.79	0.87	0.05	$260E-5$
40	0.67	0.63	0.14	$60.8E-5$
50	0.62	0.70	0.18	$17.7E-5$
60	0.67	0.68	0.18	$6.45E-5$
70	0.63	0.81	0.19	$2.35E-5$

temperatures, as shown in Figure 10. The data were found to be in agreement with the Arrhenius equation:

$$f_{\max}(T) = f_{\infty} \exp\left(-\frac{E_A}{k_\beta T}\right), \quad (8)$$

where f_{∞} represents the preexponential factor, E_A represents the activation energy, and k_β represents the Boltzmann constant. It can be seen that both processes follow Arrhenius' law, with activation energies of 1.2 eV and 1.6 eV for the Maxwell-Wagner-Sillars and dipolar relaxation, respectively.

It is evident from Figure 11 that the values of the relaxation rate $f_{\max}$ of Maxwell-Wagner-Sillars are significantly influenced by the structure of the nanocomposites, with the values of $f_{\max}$ being higher in the well-dispersed PE/O-MMT/PE-MA nanocomposites than in the PE/O-MMT nanocomposites. In order to better understand the relationship between the structure and the relaxation rate $f_{\max}$ of the Maxwell-Wagner-Sillars relaxation process, Böhning et al. [14] suggest

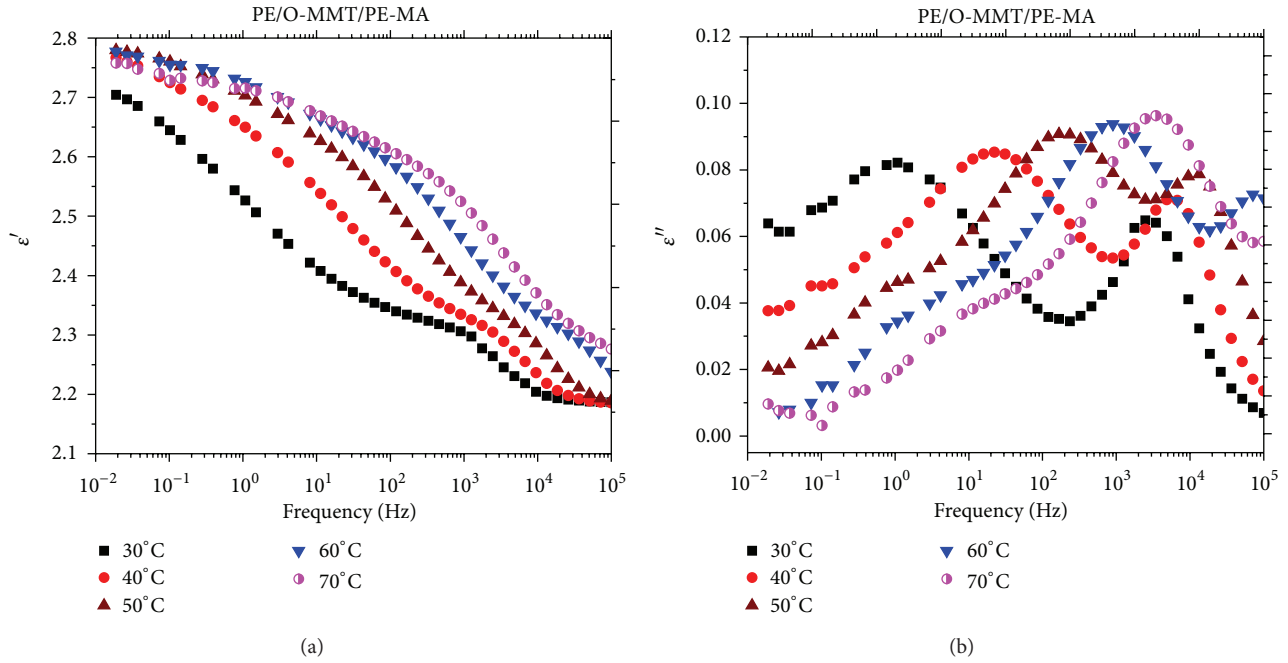

FIGURE 9: Relative permittivity ε' (a) and dielectric loss ε'' (b) for PE/O-MMT/PE-MA nanocomposites versus frequency at different temperatures.

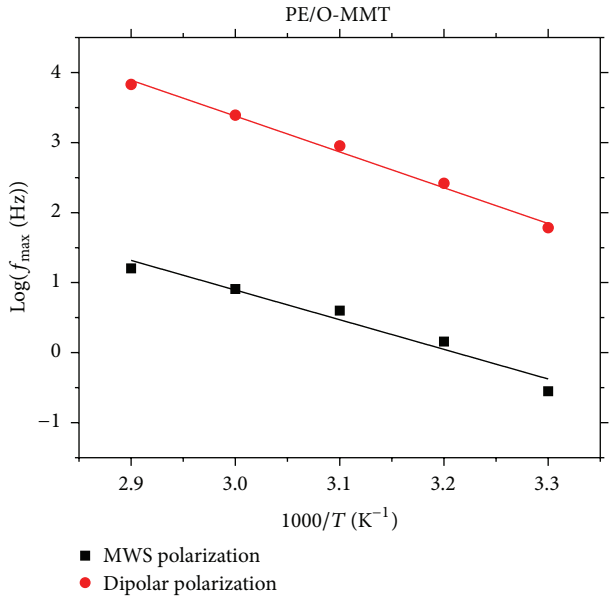

FIGURE 10: Relaxation rate f_{max} as a function of inverse temperature for the two relaxation modes observed in PE/O-MMT nanocomposites. The solid lines represent best fits for the Arrhenius function.

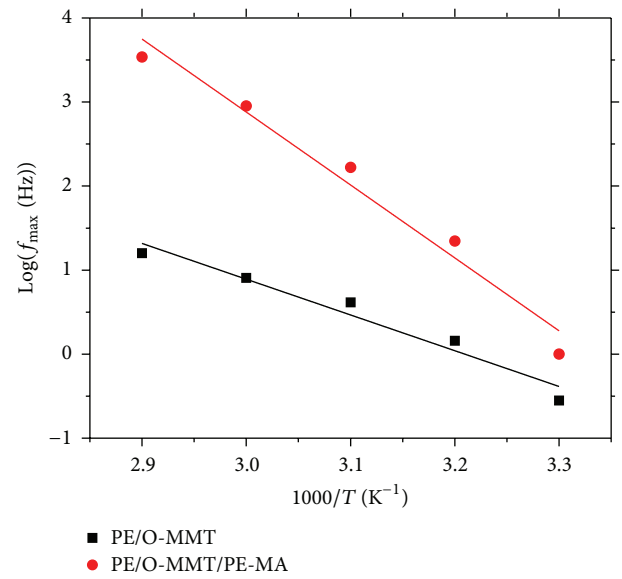

FIGURE 11: Relaxation rate f_{max} as a function of inverse temperature for the MWS relaxation rate observed in PE/O-MMT and PE/O-MMT/PE-MA nanocomposites. The solid lines represent best fits for the Arrhenius function.

that f_{max} is inversely proportional to the mean distance d between separated nanoclay layers:

$$\frac{f_{max\,2}}{d_1} \approx \frac{f_{max\,1}}{d_2}. \quad (9)$$

Accordingly, the improvement in the degree of dispersion in PE/O-MMT/PE-MA nanocomposites obtained with the addition of the compatibilizer leads to a decrease in the mean distance between the clay layers and consequently an increase in the relaxation rate f_{max} for the Maxwell-Wagner- Sillars process.

5. Conclusion

A commercially available premixed polyethylene/O-MMT masterbatch was used in this study to prepare PE/O-MMT nanocomposites using a corotating twin-screw extruder.

The quality of dispersion was improved by the incorporation of anhydride modified polyethylene (PE-MA) as the compatibilizer. This is due to the fact that PE-MA helps polymer chains to penetrate the galleries of the organoclay easily. No relaxation processes were observed in the neat PE, but two thermally activated relaxation modes were observed in the nanocomposite materials: a low-frequency relaxation that can be attributed to an interfacial process and a high-frequency relaxation that is related to a dipolar polarization process. It was observed that the relaxation rate of the Maxwell-Wagner-Sillars process increased as the degree of dispersion increased. This correlation shows that broadband dielectric spectroscopy can be used as a macroscopic tool to evaluate the quality of dispersion in nanocomposite materials.

Conflict of Interests

The authors declare that there is no conflict of interests regarding the publication of this paper.

Acknowledgment

The authors are grateful for the financial support revived from the National Sciences and Engineering Research Council of Canada (NSERC).

References

[1] M. Kawasumi, N. Hasegawa, M. Kato, A. Usuki, and A. Okada, "Preparation and mechanical properties of polypropylene-clay hybrids," *Macromolecules*, vol. 30, no. 20, pp. 6333–6338, 1997.

[2] H. Tan and W. Yang, "Toughening mechanisms of nanocomposite ceramics," *Mechanics of Materials*, vol. 30, no. 2, pp. 111–123, 1998.

[3] Y. Han, Z. Wang, X. Li, J. Fu, and Z. Cheng, "Polymer-layered silicate nanocomposites: synthesis, characterization, properties and applications," *Current Trends in Polymer Science*, vol. 6, pp. 1–16, 2001.

[4] X. Kornmann, H. Lindberg, and L. A. Berglund, "Synthesis of epoxy-clay nanocomposites: influence of the nature of the clay on structure," *Polymer*, vol. 42, no. 4, pp. 1303–1310, 2001.

[5] L. A. Utracki and M. R. Kamal, "Clay-containing polymeric nanocomposites," *Arabian Journal for Science and Engineering*, vol. 27, no. 1, pp. 43–67, 2002.

[6] S. Hotta and D. R. Paul, "Nanocomposites formed from linear low density polyethylene and organoclays," *Polymer*, vol. 45, no. 22, pp. 7639–7654, 2004.

[7] K. Zhao and K. He, "Dielectric relaxation of suspensions of nanoscale particles surrounded by a thick electric double layer," *Physical Review B*, vol. 74, no. 20, Article ID 205319, 10 pages, 2006.

[8] H. Awaji, Y. Nishimura, S. Choi, Y. Takahashi, T. Goto, and S. Hashimoto, "Toughening mechanism and frontal process zone size of ceramics," *Journal of the Ceramic Society of Japan*, vol. 117, no. 1365, pp. 623–629, 2009.

[9] L. Chen and G. Chen, "Relaxation behavior study of silicone rubber crosslinked network under static and dynamic compression by electric response," *Polymer Composites*, vol. 30, no. 1, pp. 101–106, 2009.

[10] P. Kim, N. M. Doss, J. P. Tillotson et al., "High energy density nanocomposites based on surface-modified $BaTiO_3$ and a ferroelectric polymer," *ACS Nano*, vol. 3, no. 9, pp. 2581–2592, 2009.

[11] M. A. Osman, J. E. P. Rupp, and U. W. Suter, "Tensile properties of polyethylene-layered silicate nanocomposites," *Polymer*, vol. 46, no. 5, pp. 1653–1660, 2005.

[12] X. Zhang, Z. Liu, Q. Li, Y. Leung, K. Ip, and S. Hark, "Routes to grow well-aligned arrays of ZnSe nanowires and nanorods," *Advanced Materials*, vol. 17, no. 11, pp. 1405–1410, 2005.

[13] R. D. Davis, A. J. Bur, M. McBrearty, Y. Lee, J. W. Gilman, and P. R. Start, "Dielectric spectroscopy during extrusion processing of polymer nanocomposites: a high throughput processing/characterization method to measure layered silicate content and exfoliation," *Polymer*, vol. 45, no. 19, pp. 6487–6493, 2004.

[14] M. Böhning, H. Goering, A. Fritz et al., "Dielectric study of molecular mobility in poly(propylene-graft-maleic anhydride)/clay nanocomposites," *Macromolecules*, vol. 38, no. 7, pp. 2764–2774, 2005.

[15] N. Noda, Y. H. Lee, A. J. Bur et al., "Dielectric properties of nylon 6/clay nanocomposites from on-line process monitoring and off-line measurements," *Polymer*, vol. 46, no. 18, pp. 7201–7217, 2005.

[16] P. J. Purohit, J. E. Huacuja-Sánchez, D. Wang et al., "Structure-property relationships of nanocomposites based on polypropylene and layered double hydroxides," *Macromolecules*, vol. 44, no. 11, pp. 4342–4354, 2011.

[17] V. Tomer, G. Polizos, C. A. Randall, and E. Manias, "Polyethylene nanocomposite dielectrics: implications of nanofiller orientation on high field properties and energy storage," *Journal of Applied Physics*, vol. 109, no. 7, Article ID 074113, 11 pages, 2011.

[18] J. Morawiec, A. Pawlak, M. Slouf, A. Galeski, E. Piorkowska, and N. Krasnikowa, "Preparation and properties of compatibilized LDPE/organo-modified montmorillonite nanocomposites," *European Polymer Journal*, vol. 41, no. 5, pp. 1115–1122, 2005.

[19] T. G. Gopakumar, J. A. Lee, M. Kontopoulou, and J. S. Parent, "Influence of clay exfoliation on the physical properties of montmorillonite/polyethylene composites," *Polymer*, vol. 43, no. 20, pp. 5483–5491, 2002.

[20] M. J. Dumont, A. Reyna-Valencia, J. P. Emond, and M. Bousmina, "Barrier properties of polypropylene/organoclay nanocomposites," *Journal of Applied Polymer Science*, vol. 103, no. 1, pp. 618–625, 2007.

[21] N. Hasegawa, M. Kawasumi, M. Kato, A. Usuki, and A. Okada, "Preparation and mechanical properties of polypropylene-clay hybrids using a maleic anhydride-modified polypropylene oligomer," *Journal of Applied Polymer Science*, vol. 67, no. 1, pp. 87–92, 1998.

[22] N. Hasegawa, H. Okamoto, M. Kato, and A. Usuki, "Preparation and mechanical properties of polypropylene-clay hybrids based on modified polypropylene and organophilic clay," *Journal of Applied Polymer Science*, vol. 78, no. 11, pp. 1918–1922, 2000.

[23] M. Kato, A. Usuki, and A. Okada, "Synthesis of polypropylene oligomer-clay intercalation compounds," *Journal of Applied Polymer Science*, vol. 66, no. 9, pp. 1781–1785, 1997.

[24] P. Maiti, P. H. Nam, M. Okamoto, N. Hasegawa, and A. Usuki, "Influence of crystallization on intercalation, morphology, and mechanical properties of polypropylene/clay nanocomposites," *Macromolecules*, vol. 35, no. 6, pp. 2042–2049, 2002.

[25] E. Manias, A. Touny, L. Wu, K. Strawhecker, B. Lu, and T. C. Chung, "Polypropylene/montmorillonite nanocomposites. Review of the synthetic routes and materials properties," *Chemistry of Materials*, vol. 13, no. 10, pp. 3516–3523, 2001.

[26] P. H. Nam, P. Maiti, M. Okamoto, T. Kotaka, N. Hasegawa, and A. Usuki, "A hierarchical structure and properties of intercalated polypropylene/clay nanocomposites," *Polymer*, vol. 42, no. 23, pp. 9633–9640, 2001.

[27] Y. Wang, F. B. Chen, K. C. Wu, and J. C. Wang, "Shear rheology and melt compounding of compatibilized-polypropylene nanocomposites: effect of compatibilizer molecular weight," *Polymer Engineering and Science*, vol. 46, no. 3, pp. 289–302, 2006.

[28] F. Kremer and A. Schönhals, *Broadband Dielectric Spectroscopy*, Springer, New York, NY, USA, 2003.

[29] E. Laredo, M. Grimau, F. Sánchez, and A. Bello, "Water absorption effect on the dynamic properties of nylon-6 by dielectric spectroscopy," *Macromolecules*, vol. 36, no. 26, pp. 9840–9850, 2003.

[30] H. M. Le Huy and J. Rault, "Remarks on the α and β transitions in swollen polyamides," *Polymer*, vol. 35, no. 1, pp. 136–139, 1994.

[31] D. W. McCall and E. W. Anderson, "Dielectric properties of linear polyamides," *The Journal of Chemical Physics*, vol. 32, no. 1, pp. 237–241, 1960.

Hindawi Publishing Corporation
Journal of Nanotechnology
Volume 2013, Article ID 279090, 4 pages
http://dx.doi.org/10.1155/2013/279090

Research Article

Rheological Behavior of Carbon Nanotubes as an Additive on Lithium Grease

Alaa Mohamed,[1,2] Aly Ahmed Khattab,[2] Tarek Abdel Sadek Osman,[2] and Mostafa Zaki[1]

[1] *Production Engineering and Printing Technology Department, Akhbar El Yom Academy, Giza 12211, Egypt*
[2] *Mechanical Design and Production Engineering Department, Faculty of Engineering, Cairo University, Giza 12211, Egypt*

Correspondence should be addressed to Alaa Mohamed; alaa_elking@hotmail.com

Received 14 July 2013; Revised 28 July 2013; Accepted 4 August 2013

Academic Editor: Hongmei Luo

The rheological behaviors of carbon nanotubes (CNTs) as an additive on lithium grease at different concentrations were examined under various settings of shear rate, shear stress, and apparent viscosity. The results indicated that the optimum content of the CNTs was 2%. These experimental investigations were evaluated with a Brookfield Programmable Rheometer DV-III ULTRA. The results indicated that the shear, stress and apparent viscosity increase with the increase of CNTs concentration. The microstructure of CNTs and lithium grease was examined by high resolution transmission electron microscope (HRTEM) and scanning electron microscope (SEM). The results indicated that the microscopic structure of the lithium grease presents a more regular and homogeneous network structure, with long fibers, which confirms the rheological stability.

1. Introduction

Grease is a solid or semifluid which would normally have been employed together with a thickener, additive, and antioxidant agent. The fluid lubricant that performs the actual lubrication can be petroleum (mineral oil), synthetic oil, or vegetable oil. The thickener gives grease its characteristic consistency and is sometimes believed as a "sponge" that holds the oil in place [1]. The majority of greases on the market are composed of mineral oil blended with a soap thickener. Additives enhance the performance and protect the grease and lubricate surfaces. The influence of the rheological properties of CNTs additives is very important for all the grease lubricating bearings. To characterize a lubricant comprehensively, the rheological properties at all working conditions, pressures, and temperatures have to be known [2]. Grease is widely used as a lubricant in the wheel assembly, journal bearings, and rolling element bearings. Grease is also used in other areas that need occasional service like the brake or stopper assembly to help keep these fittings rust-free and make removal of dirt and grime easier. Grease is applied to machines that can be lubricated infrequently and where lubricating oil would not stay in position. It also acts as a barrier to prevent entering of water and the incompressible materials. CNTs used as a performance enhancing additive in gear lubricants for extended lifetimes, lower operating costs, and improved power efficiency. Numerous laboratory investigations and industrial experience indicate that using of CNTs has significant advantages compared to conventional solid lubricants in both mild and extreme pressure conditions.

Lubricating grease consistency has been evaluated for years with cone penetration test ASTM-D217. The test measures the distance in tenths of a millimeter to which a standard metal cone will penetrate into the grease surface under standard conditions. This single numerical value has been proven to be inadequate to estimate the real consistency of lubricating grease under dynamic conditions. It ignores the non-Newtonian flow behavior characteristic to grease. In the past few years, rheology has been introduced as a new method to better understand and evaluate the real behavior of lubricating grease. Rheology takes into account the influence of shear rate, shear stress, temperature, and time. By measuring the viscosity with both rotational and capillary rheometer, it is possible to see the effect of shear rate on grease consistency which strongly influences the lubricating capability of greases under load [3].

The aim of this work is to evaluate the rheological behaviors of carbon nanotubes (CNTs) as an additive on lithium

Table 1: Composition of the tested grease.

Base oil	Mineral oil
Soap thickener	Lithium
Penetration (1/10 mm at 25°C)	280
Dropping point	180°C
Viscosity of base oil at 40°C	150 cSt

grease at different concentrations and study the microstructure of lithium grease.

2. Experimental Methodology

2.1. Syntheses of Carbon Nanotubes and Lithium Grease. CNTs were synthesized by the electric arc discharge. The arc is generated between two electrodes (size φ 6 × 100 mm) using distilled water. The cathode and the anode are from graphite (99.9% pure) and was performed under AC current, 75 A and 238 V.

Grease that was used in this work was commercially available; the main physical-chemical properties of the grease are presented in Table 1. The grease is lithium based and has good heat resistance, water resistance, and mechanical stability. In order to study the rheological behavior of carbon nanotubes as an additives on lithium grease, carbon nanotubes were added into lithium grease at different concentrations (0.5, 1, 2, and 3 wt.%). The carbon nanotube particles were dispersed well in the grease in an ultrasonic bath.

2.2. Structural Characterization. The size and morphology of carbon nanotube were characterized with high resolution transmission electron microscopy (HRTEM) (JEOL JEM 2100) with an accelerating voltage of 200 kV.

The grease structure was investigated by a (JEOL JSM-5600LV) scanning electron microscope (SEM) with an accelerating voltage of 30 kV, resolution of 3.5 nm, probe current of (10^{-12} to 10^{-6}) A.

2.3. Viscometer (Brookfield Programmable Rheometer DV-III Ultra). Rheological measurements were performed on a Brookfield Programmable Rheometer DV-III ultra used in conjunction with Brookfield software, RHEOCALC V.2. Through RHEOCALC, all rheometer functions (rotational speed, instrument % torque scale, time interval, and set temperature) are controlled by a computer. The corresponding shear stress, shear rate, dynamic viscosity, mathematical model, confidence of fit, and the consistency index were also recorded through the software. The temperature was controlled by connection with bath controller HT-107 and measured by the attached temperature probe.

The Brookfield DV-III Ultra Programmable Rheometer measures fluids and semifluid parameters of shear stress and apparent viscosity at given shear rates. The principle of operating the DV-III Ultra is to drive a spindle (which is immersed into the test fluid) through a calibrated spring. The viscous drag of the fluid against the spindle is measured by the spring deflection. Spring deflection is measured with a rotary transducer. The viscosity measurement range of the DV-III Ultra (in centipoises or CP) is determined by the rotational speed of the spindle, the size and shape of the spindle, the container in which the spindle is rotated, and the full scale torque of the calibrated spring. The schematic of the instrument is illustrated in Figure 1.

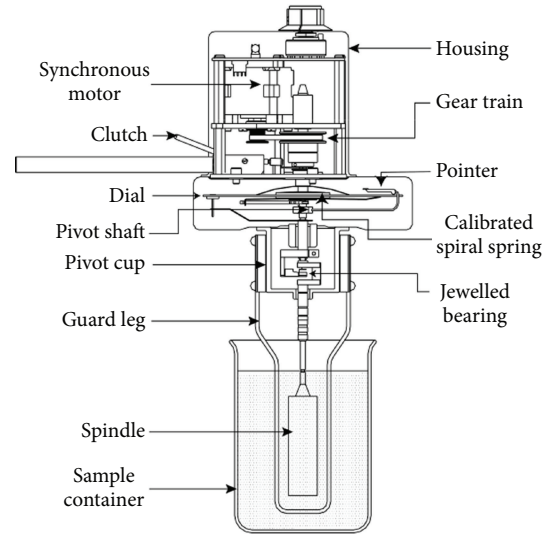

Figure 1: The principle of Brookfield DV-III ultra.

Before carrying out measurements, rheometer DV-III Ultra is turned on, leveled, and autozeroed. The level is adjusted using the three feet on the bottom of the base and confirmed by the bubble on the top of the head. The feet are adjusted until the bubble is inside the center target and sets the level prior to autozero. All measurements have been carried out with cone radius 24 mm and with 0.8° cone angle; this gives the gap height of 0.1 mm at the circumference of the cone.

3. Results and Discussion

3.1. Structural Characterization of Carbon Nanotubes. High resolution transmission electron microscope (HRTEM) image of CNTs shown in Figure 2 shows the presence of different structures in the sample and that the average size of the nanoparticles is about 10 nm in diameter and 1–25 μm in length.

Figure 3 shows the SEM image of CNTs dispersed in lithium hydroxystearate (soap) fiber. It can be seen that there is no apparent aggregation of CNTs, indicating that the CNTs could be well dispersed in lithium grease, and it can be observed that the microscopic structure of lithium grease presents a more regular and homogeneous network structure, with long fibers, which confirm the rheological stability.

3.2. Rheological Behavior of Carbon Nanotubes as an Additives on Lithium Grease. Many models are available to describe rheological properties of lithium grease such as Bingham model, Herschel-Bulkley model, Casson model, Bauer model,

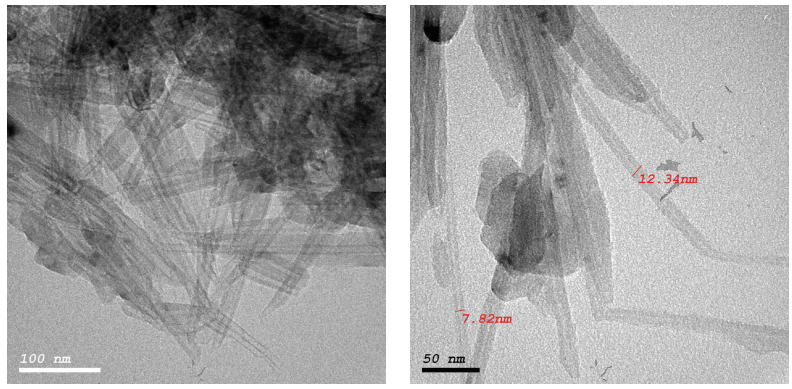

(a) (b)

Figure 2: HRTEM images of CNTs.

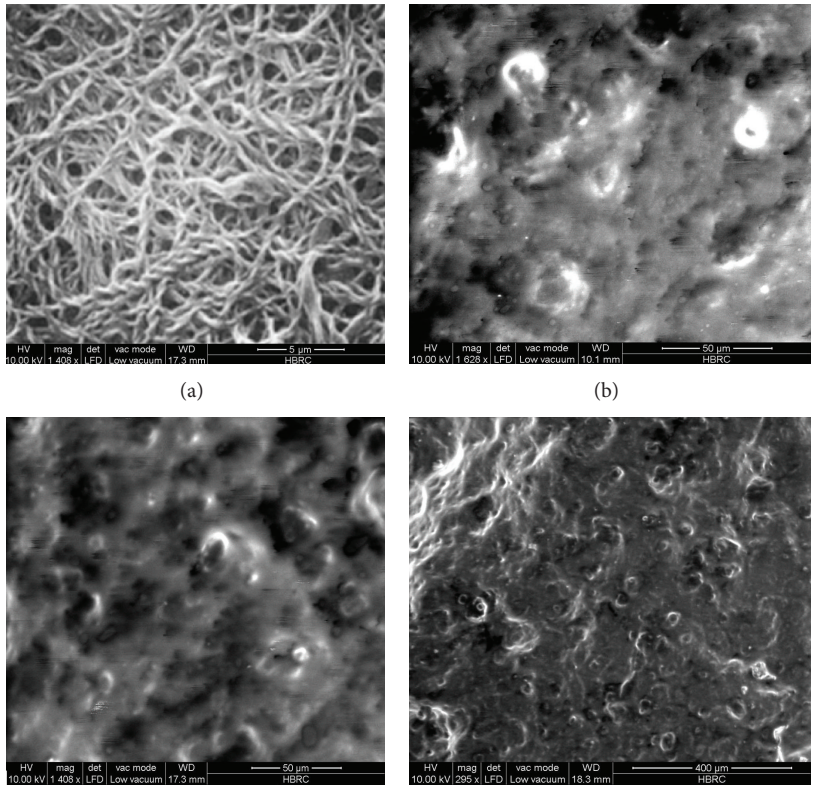

(a) (b)

(c) (d)

Figure 3: SEM image of grease with (a) base grease, (b) 0.5% CNTs, (c) 1% CNTs, and (d) 2% CNTs.

Balan model, Papanastasiou model, and Dorier and Tichy model.

The rheological results from the measurements with the cone and plate rheometer, that are shown in Figures 4 and 5 represent the effect of carbon nanotube additives on lithium grease with shear stress and viscosity.

Figures 4 and 5 give the shear stress and apparent viscosity as a function of shear rate for lithium grease alone and that containing different concentrations (0.5, 1, 2, and 3 wt.%) of CNTs. It can be seen that the shear stress and apparent viscosity of the lithium grease containing 2 wt.% CNTs are much higher and more stable than that of pure lithium grease at all shear rates. At this point, the shear stress and apparent viscosity could be increased by 67.3% and 81.8%, respectively. The shear stress of base grease and the grease containing CNTs becomes larger with the increase of shear rate and with the increase of the percentage of carbon nanotube additives on lithium grease.

The apparent viscosity of base grease and the grease containing CNTs becomes larger with the decrease of shear rate

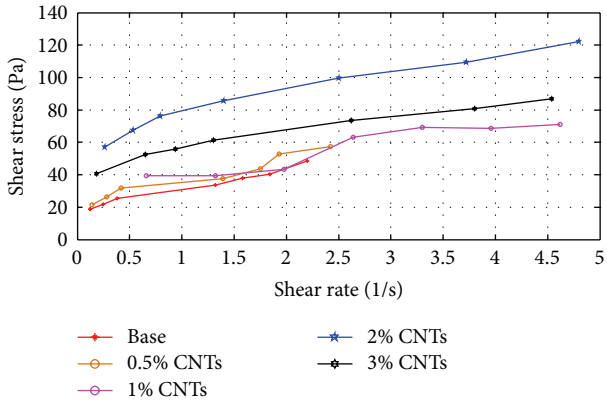

Figure 4: Shear stress of the grease samples.

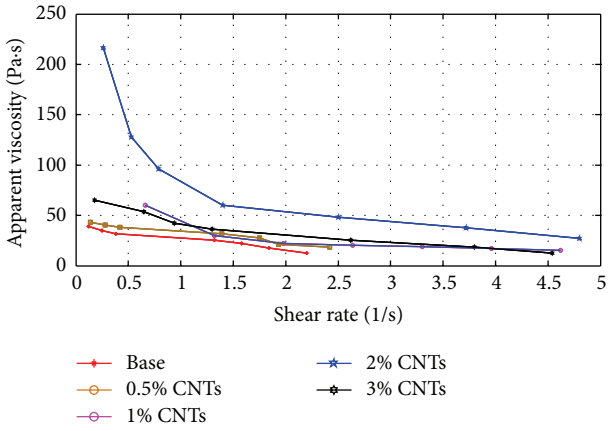

Figure 5: Apparent viscosity of the grease samples.

and increases with increasing the percentage of carbon nanotube additives on lithium grease. These experiments were carried out under stationary conditions, to avoid thixotropic behavior. Therefore, the result indicates that all the samples show a large shear thinning behaviour. At low strain rates, the values of apparent viscosity follow quite well the classification found for the yield stress.

4. Conclusions

According to the above results and discussion, the conclusions can be summarized as follows.

(1) CNTs were successfully synthesized by electric arc discharge method. The synthesized CNTs have an average diameter of 10 nm and could be well dispersed in lithium grease.

(2) A rheological characterization, including apparent viscosity, shear stress, and shear rate, was carried out at different concentrations of CNTs. The grease response was studied at constant temperature and time, which led to a real mechanical spectroscopic investigation.

(3) The microstructure of lithium grease at different concentrations was confirmed by scanning electron microscope (SEM). The results indicated that the microscopic structure of the lithium grease presents a more regular and closer network structure with long fibers, which confirms the rheological stability.

(4) This paper confirms the importance of the correlation between rheological properties and the grease microscopic structure.

(5) Finally, the optimum percentage of the CNTs in the grease composites was 2%.

References

[1] F. Chinas-Castillo and H. A. Spikes, "The behavior of colloidal solid particles in Elastohydrodynamic contacts," *Tribology Transactions*, vol. 43, no. 3, pp. 387–394, 2000.

[2] A. V. Radulescu and I. Radulescu, "Rheological models for lithium and calcium greases," *Mechanika*, vol. 59, no. 3, pp. 67–70, 2006.

[3] K. Siik and J. Vuorinen, "The influence of shear thinning behavior on lubricating grease consistency and its effect on oil separation," in *Proceedings of the Annual Transactions of the Nordic Rheology Conference*, S. L. Mason, Ed., vol. 13, pp. 247–248, The Nordic Rheology Society, Tampere, Finland, June 2005.

Hindawi Publishing Corporation
Journal of Nanotechnology
Volume 2013, Article ID 598328, 5 pages
http://dx.doi.org/10.1155/2013/598328

Research Article

Synthesis and Characterization of Silver Nanoparticles Using Cannonball Leaves and Their Cytotoxic Activity against MCF-7 Cell Line

Preetha Devaraj,[1] Prachi Kumari,[1] Chirom Aarti,[1] and Arun Renganathan[2]

[1] *Department of Biotechnology, Faculty of Science Humanities, SRM University, Kattankulathur 603 203, Chennai, Tamil Nadu, India*
[2] *Department of Biomedical Science, School of Basic Medical Sciences, Bharathidasan University, Tiruchirappalli 620 024, Tamil Nadu, India*

Correspondence should be addressed to Preetha Devaraj; preethad06@gmail.com

Received 7 May 2013; Accepted 8 July 2013

Academic Editor: Hongmei Luo

Cannonball (*Couroupita guianensis*) is a tree belonging to the family Lecythidaceae. Various parts of the tree have been reported to contain oils, keto steroids, glycosides, couroupitine, indirubin, isatin, and phenolic substances. We report here the synthesis of silver nanoparticles (AgNPs) using cannonball leaves. Green synthesized nanoparticles have been characterized by UV-Vis spectroscopy, SEM, TEM, and FTIR. Cannonball leaf broth as a reducing agent converts silver ions to AgNPs in a rapid and ecofriendly manner. The UV-Vis spectra gave surface plasmon resonance peak at 434 nm. TEM image shows well-dispersed silver nanoparticles with an average particle size of 28.4 nm. FTIR showed the structure and respective bands of the synthesized nanoparticles and the stretch of bonds. Green synthesized silver nanoparticles by cannonball leaf extract show cytotoxicity to human breast cancer cell line (MCF-7). Overall, this environmentally friendly method of biological silver nanoparticles production provides rates of synthesis faster than or comparable to those of chemical methods and can potentially be used in various human contacting areas such as cosmetics, foods, and medical applications.

1. Introduction

Couroupita guianensis, whose common names include ayahuma and the cannonball tree, is an evergreen tree allied to the Brazil nut (*Bertholletia excelsa*) and is native to tropical northern South America and to the southern Caribbean. As per textual record, the tree has been growing for the past three thousand years in India. The cannonball tree possesses many medicinal properties such as antibiotic, antifungal, antiseptic, and analgesic qualities. Extracts of this tree were used to cure colds and stomach aches. Juice made from the leaves is used to cure skin diseases and malaria. The inside of the fruit can disinfect wounds and young leaves ease toothache. The fruit emits an unpleasant odour and can be used as an insect repellent just by rubbing it to the skin or clothes [1, 2]. Overall the tree possesses skin fibroblast proliferation, antioxidant [3, 4], antihelmintic [5], wound healing, antimicrobial, and antinociceptive [1] activities.

Nanotechnology is significant on account of its preeminence upon the comprehension, use, and control of matter at magnitudes of a minute scale, akin to approaching atomic levels, with which to manufacture new substances, instruments, and frameworks [6]. The synthesis of nanocrystals is in the limelight in modern nanotechnology. Biosynthesis of nanoparticles by plant extracts is currently under exploitation [7]. Nanotechnology is currently employed as a tool to explore the darkest avenues of medical sciences in several ways like imaging [8], sensing [9], targeted drug delivery [10], gene delivery systems [11], and artificial implants [12].

In present situation, silver nanoparticles (AgNPs) are in great use in the medicinal, pharmaceutical, agricultural industry and in water purification. These nanoparticles can

be synthesized either chemically or biologically. But the chemical process for synthesis of silver nanoparticles is more elaborate and leaves behind toxic effect that adversely affects the ecosystem. On the other hand, biological synthesis of silver nanoparticles is less time consuming, less costly, and more ecofriendly; therefore, in recent time, scientists are looking forward to the possible biological methods for the synthesis of silver nanoparticles [13]. AgNPs have unique optical, electrical, and thermal properties and are being incorporated into products that range from photovoltaics to biological and chemical sensors. Examples include conductive inks, pastes, and fillers which utilize silver nanoparticles for their high electrical conductivity, stability, and low sintering temperatures; in addition, AgNPs are applied in molecular diagnostics and photonic devices. An increasingly common application is the use of silver nanoparticles for antimicrobial coatings, and many textiles, keyboards, wound dressings, and biomedical devices now contain silver nanoparticles that continuously release a low level of silver ions to provide protection against bacteria. In the present study, the green synthesis of silver nanoparticles from the cannonball leaf extract has been carried out and characterized by UV-Vis spectra, SEM, TEM, and FTIR analysis. The cytotoxicity activity of synthesized AgNPs against MCF-7 breast cancer cell line was determined.

2. Experimental

2.1. Preparation of Leaf Extract for Silver Nanoparticles. Cannonball leaves were collected and washed twice with distilled water and dried at 40°C. Dried leaves were finely powdered in an electric grinder and stored at room temperature in an airtight container till further use.

2.1.1. Aqueous Extract. Ten grams of dried powder of cannonball leaves was added to 100 mL of distilled water and stirred for 6 h at slow heat. Every two hours the contents were filtered through eight layers of muslin cloth, and the filtrate was centrifuged at 5000 rpm for 15 min. This process was repeated twice, and the supernatant was pooled and concentrated by using a rotary vacuum evaporator at reduced pressure. The concentrated extract was sterilized and stored at 4°C.

2.1.2. Solvent Extract. Ten grams of dried powder of cannonball leaves was extracted with 100 mL of ethanol, acetone, petroleum ether, and chloroform, respectively, kept on a rotator shaker at 190–220 rpm for 24 h. The contents were filtered through eight layers of muslin cloth and the filtrate was centrifuged at 5000 rpm for 15 min. This process was repeated twice, and the supernatant was pooled and concentrated by using a rotary vacuum evaporator at reduced pressure. The concentrated extract was sterilized and stored at 4°C till further studies.

2.2. Synthesis of AgNPs. The synthesis of silver nanoparticles was done by mixing cannonball leaf extract and 1 mM of aqueous silver nitrate solution ($AgNO_3$) in the ratio 1 : 10 and heated at 80°C until the color of the solution was changed from brown to reddish brown. At this point the solution was cooled to room temperature and centrifuged at 5000 rpm for 10 minutes. The supernatant was discarded and the pellet was air dried in the incubator.

2.3. Characterization of AgNPs. UV-absorption spectra of synthesized AgNPs by using cannonball leaf extract were measured using UV-visible spectrometer (Shimadzu UV-2700). Scanning electron microscopy (SEM) analysis of synthesized AgNPs was done using a Hitachi S-4500 SEM machine. The size and shape of the synthesized AgNPs were determined by transmission electron microscopy (TEM). The TEM images of synthesized AgNPs were obtained by using TECHNAI 10 Philips. Prior to analysis, AgNPs were sonicated for 5 minutes, and a drop of appropriately diluted sample was placed onto a carbon-coated copper grid. The liquid fraction was allowed to evaporate at room temperature. Fourier transform infrared (FTIR) spectral measurements were carried out to identify the potential biomolecules in cannonball leaf extract which is responsible for reducing and capping the bioreduced silver nanoparticles.

2.4. Cytotoxicity of AgNPs. The cytotoxicity of synthesized AgNPs against MCF-7 cells was measured by MTT (3-(4, 5-dimethylthiazol-2-yl)-2, 5-diphenyl tetrazolium bromide) assay. The MTT assay is a colorimetric, nonradioactive assay for measuring cell viability through increased metabolization of tetrazolium salt [14]. MCF-7 cells were seeded at a density of 5×10^4 cells/well into 96-well plates. Then, the cells were treated with different concentration of synthesized AgNPs (0–100; μL/mL) and incubated in the presence of 5% CO_2 and 95% humidity at 37°C for 24 h. MTT (5 mg/mL) was added to the incubated cells, then incubated further for another 4 h. The crystals were dissolved in 200 μL of DMSO and the absorbance was measured colorimetrically at 570 nm with reference filter as 655 nm.

3. Results and Discussion

In the present study, reduction of silver ions present in the aqueous solution of silver nitrate during the reaction with the ingredients of cannonball leaf extract has been seen by the UV-Vis spectroscopy ranging from 300 to 600 nm. The maximum absorption was obtained at 440 nm (Figure 1). The bioreduction of $AgNO_3$ ions in solution was monitored by periodic sampling of aliquots (0.1 mL) of aqueous component and measuring UV-Vis spectra of the solution. UV-Vis spectra show no evidence of absorption in the range of 400–800 nm for the plant extract (Figure 1(a)), and the plant extract solution exposed to $AgNO_3$ ions shows a distinct absorption at around 434 nm (Figure 1(b)) which corresponds to surface plasmon resonance (SPR) of silver nanoparticles established at 420 nm in previous studies [15]. It is observed that the silver SPR band occurs initially at 430 nm; after completion of the reaction, the wavelength of the SPR band stabilizes at 434 nm. Green synthesized AgNPs were stable for six months without shifting the surface plasmon absorbance band [16, 17]. This

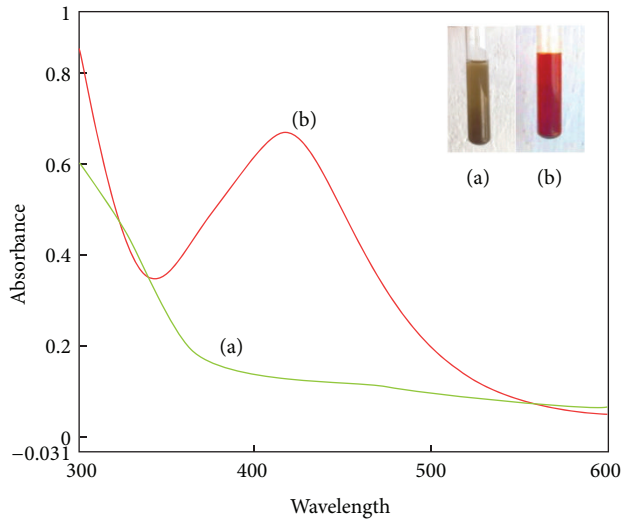

Figure 1: UV-Vis absorption spectrum of (a) cannonball leaf extract and (b) biosynthesized AgNPs.

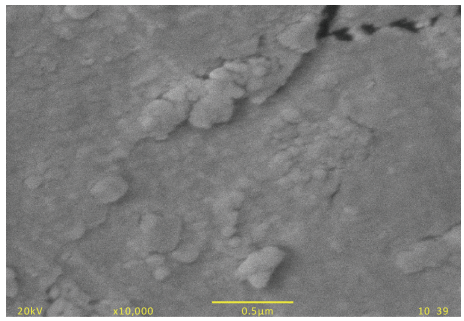

Figure 2: SEM micrograph of AgNPs synthesized from cannonball leaf extract.

suggests that the phytochemical present in cannonball leaves acts as a reducing agent.

SEM analysis shows high-density AgNPs synthesized by cannonball leaf extract (Figure 2). It was shown that relatively spherical and uniform AgNPs were formed with diameter of 13 to 61 nm. The SEM image of silver nanoparticles was due to interactions of hydrogen bond and electrostatic interactions between the bioorganic capping molecules bound to the AgNPs. The nanoparticles were not in direct contact even within the aggregates, indicating stabilization of the nanoparticles by a capping agent [18]. The larger silver particles may be due to the aggregation of the smaller ones, due to the SEM measurements.

Figure 3 shows the TEM image of AgNPs synthesized by using cannonball leaf extract which predominates with spherical triangle, truncated triangles, and decahedral morphologies ranging from 25 to 40 nm with an average size of 28.40 nm. Most of the AgNPs were roughly circular in shape with smooth edges. These structures were identical with those of the Ag nanoparticles produced from the extract prepared from leaves of *Cinnamomum camphora* and phyllanthin, which was attributed to a similarity in the reductive agents present in both plant species [6, 19]. The phytochemical constituents in the cannonball leaves such as tannins, phenols, saponins, and flavonoids may act as reducing agents during the synthesis of AgNPs [20, 21].

The IR spectra provided information about the local molecular environment of the organic molecules on the surface of nanoparticle. In the present work, FTIR spectral measurements were carried out to identify the potential biomolecules in cannonball leaf extract which is responsible for reducing and capping the bioreduced silver nanoparticles. Fourier transform infrared spectroscopy (FTIR) is a technique which is used to analyze the chemical composition of many organic chemicals, polymers, paints, coatings, adhesives, lubricants, semiconductor materials, coolants, gases, biological samples, inorganics, and minerals. FTIR can be used to analyze a wide range of materials in bulk or thin films, liquids, solids, pastes, powders, fibres, and other forms. FTIR analysis can give not only qualitative (identification) analysis of materials, but, with relevant standards, can be used for quantitative (amount) analysis. FTIR can be used to analyze samples up to ~11 millimetres in diameter and either measure in bulk or the top ~1 micrometer layer. FTIR measurements were carried out to identify the possible biomolecules responsible for capping and efficient stabilization of the metal nanoparticles synthesized by cannonball leaf extract.

The results of FTIR analysis of this study show different stretches of bonds shown at different peaks; 3432.94—N–H stretch, 2777.28—single aldehyde, 2676.19—C–H; O–H, 2071.75—C≡C, 1637.58—C=C, and 1121.56—C=O. Figure 4 shows the peaks near 3440 cm^{-1}, 2924 cm^{-1}, and 2854 cm^{-1} assigned to OH stretching and aldehydic C–H stretching, respectively. The weaker band at 1629 cm^{-1} corresponds to amide I arising due to carbonyl stretch in proteins. The peak at 1041 cm^{-1} corresponds to C–N stretching vibration of the amine. The peak near 1741 cm^{-1} corresponds to C=C stretching (nonconjugated). The peak near 833 cm^{-1} assigned to C=CH_2 and the peaks near 677 cm^{-1} and 651.96 cm^{-1} assigned to CH out of plane bending vibrations are substituted ethylene systems –CH=CH (cis) [18]. FTIR spectra of silver nanoparticles exhibited prominent peaks at 2,927, 1,631, and 1,383 cm^{-1}. The spectra showed sharp and strong absorption band at 1,631 cm^{-1} assigned to the stretching vibration of (NH) C=O group. The band 1,383 developed for C–C and C–N stretching; presence of the sharp peak at 2,927 cm^{-1} was assigned to C–H and C–H (methoxy compounds) stretching vibration, respectively [22].

The cytotoxic activity of AgNPs synthesized by using cannonball leaf extract was determined by MTT assay (Figure 5). In the present study, the minimum inhibitory concentration (IC_{50}) of AgNPs on MCF-7 cells was obtained at 20 μL/mL at 24 hours. Exposure to increasing concentration of AgNPs shows dose-dependent cytotoxicity on MCF-7 cells. Our study correlates with the results of an earlier study [23] where *Sapium* leaves showed the highest cytotoxic activity against HeLa cell line. Cannonball leaves have also been reported to have antioxidant activity, and this may have a role to play in the observed activity in the cancer cell lines as antioxidants play a complex role in cancer prevention [24].

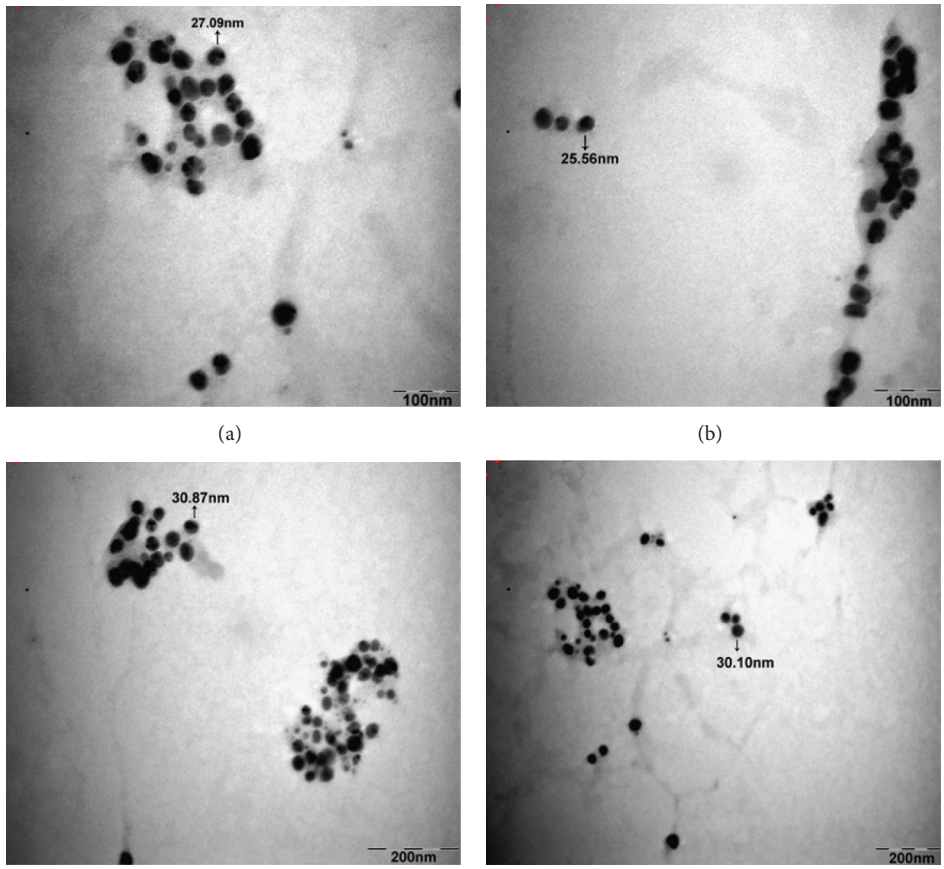

Figure 3: Transmission electron microscopy images of AgNPs at different magnification levels ((a) and (b)—100 nm; (c) and (d)—200 nm).

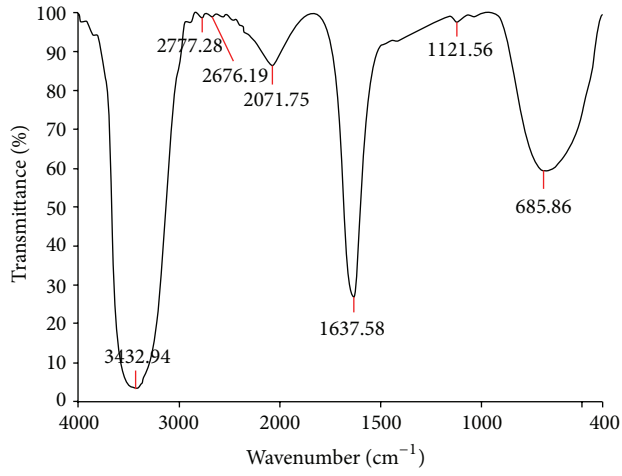

Figure 4: FTIR spectra of cannonball leaf extract.

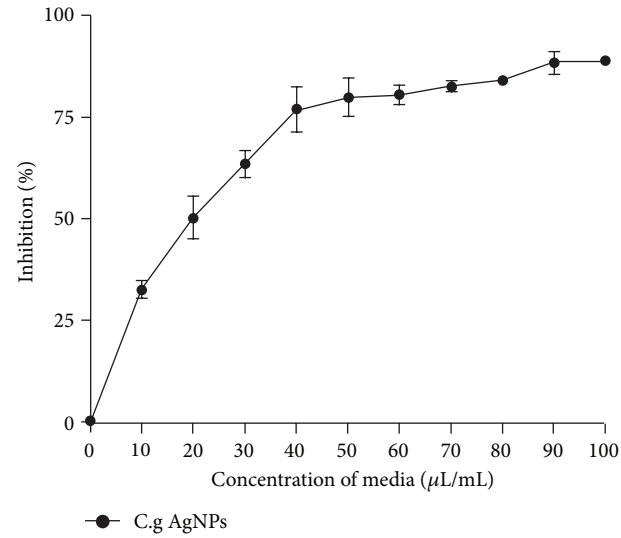

Figure 5: Cytotoxicity of synthesized AgNPs on MCF-7cells.

4. Conclusions

In conclusion, there has been an exponentially increasing interest in biological synthesis of AgNPs. In this study, AgNPs were synthesized by an ecofriendly and convenient method using cannonball leaf extract at ambient temperature. Cannonball leaf extract has been used as a reducing agent for the synthesis of silver nitrate into silver nanoparticles. Green synthesized silver nanoparticles are confirmed by color change which was monitored quantitatively by UV-Vis

spectroscopy at 440 nm. Further characterization with SEM and TEM analysis shows the spherical, polydisperse AgNPs of particle size ranging from 5 to 35 nm with an average size of 28.40 nm. FTIR showed the structure, the respective bands of the synthesized nanoparticles, and the stretch of bonds. The cytotoxicity analysis of the green synthesized silver nanoparticles was observed that it inhibits the MCF-7 breast cancer cell line. However, further investigations were needed to identify the scaling-up usage of this extract on metallic nanoparticle synthesis and its applications on anticancer therapy.

Acknowledgments

The authors would like to acknowledge their dear colleagues for their support rendered. The authors extend their heartfelt regards to the management and Director of Faculty of Science Humanities, SRM University, for their constant support throughout the research work. The authors extend their indebted thanks to TANUVAS for the help rendered in microscopic characterization.

References

[1] P. U. Sanjay, K. N. Jayaveera, C. K. Ashock Kumar, and G. S. Kumar, "Antimicrobial, wound healing and antioxidant potential of *Couroupita guianensis* in rats," *Pharmacologyonline*, vol. 3, no. 6, pp. 269–281, 2007.

[2] M. M. G. Pinheiro, S. O. Bessa, C. E. Fingolo et al., "Antinociceptive activity of fractions from *Couroupita guianensis* Aubl. leaves," *Journal of Ethnopharmacology*, vol. 127, no. 2, pp. 407–413, 2010.

[3] C. Castelluccio, G. Paganga, N. Melikian et al., "Antioxidant potential of intermediates in phenylpropanoid metabolism in higher plants," *FEBS Letters*, vol. 368, no. 1, pp. 188–192, 1995.

[4] F. Aqil, I. Ahmad, and Z. Mehmood, "Antioxidant and free radical scavenging properties of twelve traditionally used Indian medicinal plants," *Turkish Journal of Biology*, vol. 30, no. 3, pp. 177–183, 2006.

[5] V. Rajamanickam, A. Rajasekaran, S. Darlin Quine et al., "Anthelmintic activity of the flower extract of *Couroupita guianensis*," *The Internet Journal of Alternative Medicine*, vol. 8, no. 1, pp. 107–111, 2009.

[6] R. P. Feynman, "There's plenty of room at the bottom," *Science*, vol. 254, no. 5036, pp. 1300–1301, 1991.

[7] J. Huang, Q. Li, D. Sun et al., "Biosynthesis of silver and gold nanoparticles by novel sundried *Cinnamomum camphora* leaf," *Nanotechnology*, vol. 18, no. 10, Article ID 105104, 2007.

[8] P. Mukherjee, A. Ahmad, D. Mandal et al., "Fungus-mediated synthesis of silver nanoparticles and their immobilization in the mycelial matrix: a novel biological approach to nanoparticle synthesis," *Nano Letters*, vol. 1, no. 10, pp. 515–519, 2001.

[9] T. Klaus-Joerger, R. Joerger, E. Olsson, and C. G. Granqvist, "Bacteria as workers in the living factory: metal-accumulating bacteria and their potential for materials science," *Trends in Biotechnology*, vol. 19, no. 1, pp. 15–20, 2001.

[10] N. Saifuddin, C. W. Wong, and A. A. N. Yasumira, "Rapid biosynthesis of silver nanoparticles using culture supernatant of bacteria with microwave irradiation," *E-Journal of Chemistry*, vol. 6, no. 1, pp. 61–70, 2009.

[11] M. Kowshik, S. Ashtaputre, S. Kharrazi et al., "Extracellular synthesis of silver nanoparticles by a silver-tolerant yeast strain MKY3," *Nanotechnology*, vol. 14, no. 1, pp. 95–100, 2003.

[12] S. Minaeian, A. R. Shahverdi, A. S. Nohi, and H. R. Shahverdi, "Extracellular biosynthesis of silver nanoparticles by some bacteria," *Journal of Sciences Islamic Azad University*, vol. 17, no. 66, pp. 1–4, 2008.

[13] S. Karthick Raja, S. Ganesh, and Avimanyu, "Evaluation of antibacterial activity of silver nanoparticles synthesized from *Candida glabrata* and *Fusarium oxysporum*," *International Journal of Medicobiological Research*, vol. 1, no. 3, pp. 130–136, 2011.

[14] T. Mosmann, "Rapid colorimetric assay for cellular growth and survival: application to proliferation and cytotoxicity assays," *Journal of Immunological Methods*, vol. 65, no. 1-2, pp. 55–63, 1983.

[15] P. Mulvaney, "Surface plasmon spectroscopy of nanosized metal particles," *Langmuir*, vol. 12, no. 3, pp. 788–800, 1996.

[16] K. Govindaraju, S. Tamilselvan, V. Kiruthiga, and G. Singaravelu, "Biogenic silver nanoparticles by *Solanum torvum* and their promising antimicrobial activity," *Journal of Biopesticides*, vol. 3, no. 1, pp. 394–399, 2010.

[17] G. Thirumurugan and M. D. Dhanaraju, "Novel biogenic metal nanoparticles for pharmaceutical applications," *Advanced Science Letters*, vol. 4, no. 2, pp. 339–348, 2011.

[18] A. M. Priya, R. K. Selvan, B. Senthilkumar, M. K. Satheeshkumar, and C. Sanjeeviraja, "Synthesis and characterization of $CdWO_4$ nanocrystals," *Ceramics International*, vol. 37, no. 7, pp. 2485–2488, 2011.

[19] J. Kasthuri, K. Kathiravan, and N. Rajendiran, "Phyllanthin-assisted biosynthesis of silver and gold nanoparticles: a novel biological approach," *Journal of Nanoparticle Research*, vol. 11, no. 5, pp. 1075–1085, 2009.

[20] R. Kavitha, P. Kamalakannan, S. Sridhar et al., "*In vitro* antimicrobial activity and phytochemical analysis of Indian medicinal plant *Couroupita guianensis* Aubl," *Journal of Chemical Pharmaceutical Research*, vol. 3, no. 6, pp. 115–121, 2011.

[21] M. Juvekar, A. Juvekar, M. Kulkarni et al., "Phytochemical and pharmacological studies on the leaves of *Couroupita guianensis* Aubl," *Planta Medica*, vol. 75, p. PJ168, 2009.

[22] S. Marimuthu, A. A. Rahuman, G. Rajakumar et al., "Evaluation of green synthesized silver nanoparticles against parasites," *Parasitology Research*, vol. 108, no. 6, pp. 1541–1549, 2011.

[23] A. Sowemimo, M. van de Venter, L. Baatjies, and T. Koekemoer, "Cytotoxic activity of selected Nigerian plants," *African Journal of Traditional, Complementary and Alternative Medicines*, vol. 6, no. 4, pp. 526–528, 2009.

[24] A. Martínez, E. Conde, A. Moure, H. Domnguez, and R. J. Estévez, "Protective effect against oxygen reactive species and skin fibroblast stimulation of *Couroupita guianensis* leaf extracts," *Natural Product Research*, vol. 26, no. 4, pp. 314–322, 2012.

Hindawi Publishing Corporation
Journal of Nanotechnology
Volume 2013, Article ID 634726, 6 pages
http://dx.doi.org/10.1155/2013/634726

Research Article

Optimizing the Processing Conditions for the Reinforcement of Epoxy Resin by Multiwalled Carbon Nanotubes

S. Arun, Mrutyunjay Maharana, and S. Kanagaraj

Department of Mechanical Engineering, Indian Institute of Technology Guwahati, Guwahati 781039, India

Correspondence should be addressed to S. Kanagaraj; kanagaraj@iitg.ernet.in

Received 31 May 2013; Accepted 6 July 2013

Academic Editor: Guifu Zou

The reinforcement of epoxy by MWCNTs is done to obtain the required properties of composites. However, the homogeneous dispersion of MWCNTs in epoxy is a critical problem. Hence, an attempt is made to optimize the processing conditions for dispersing the MWCNTs in epoxy by solvent dispersion technique. The epoxy/MWCNTs mixture was prepared using three methods: (1) magnetic stirring at 55°C, (2) hot air oven process at 55°C, and (3) vacuum oven process at room temperature. The nanocomposites having 0.1 and 0.2 wt.% of MWCNTs were prepared, for each method. The mechanical properties of nanocomposites were studied as per ASTM-D695, and the thermal conductivity was measured using KD2 probe. It is observed that the compressive strength, Young's modulus, and thermal conductivity of 0.2 wt.% of MWCNTs prepared by vacuum oven method were found to be enhanced by 39.4, 10.7, and 59.2%, respectively, compared to those of pure epoxy. Though the properties of nanocomposites were increased with MWCNTs' concentration irrespective of the processing techniques, the vacuum-processed sample showed the most enhanced properties compared to any other method. It is concluded that a unique method for the dispersion of MWCNTs in epoxy is the solvent dispersion technique with vacuum drying process.

1. Introduction

The usage of nanoparticles as the reinforcement in a polymer matrix is increased enormously to achieve the required properties of composites. Among all the fillers such as TiO_2, ZrO_2, and nanoclay, multiwalled carbon nanotubes (MWCNTs) were paid a lot of attention because of their attractive mechanical properties which were reported by Gojny et al. [1]. Good aspect ratio of MWCNTs with the specific surface area of 1300 m^2/g helps in effective stress transfer from the matrix, which was studied by Yu et al. [2]. The desirable properties of MWCNTs made them a candidate for reinforcing the polymer matrix. Kim et al. [3] found that the homogenous dispersion of the MWCNTs which gives good interaction between the matrix and the reinforcement must be ensured, in order to achieve the improved properties of epoxy/MWCNTs nanocomposites. Starkova et al. [4] also evaluated the mechanical properties of the epoxy-based composites. The enhancement of Young's modulus of 0.1 wt.% composites was found to be 2% compared to that of pure epoxy. Mahfuz et al. [5] studied the influence of MWCNTs in epoxy, and it was found that the mechanical and thermal properties of the composites were increased. It was observed by He and Tjong [6] that the homogeneous dispersion of reinforcement was confirmed with an increase of electrical conductivity of the composites. It is observed from the previous studies that the dispersion of reinforcement is one of the most important factors in deciding the enhancement of mechanical, thermal, and electrical properties of composites.

Apart from the dispersion, the functionalization of MWCNTs is also an important factor. The functionalization of MWCNTs increased the stress transfer at the interface of the matrix and MWCNTs, and it also helped to reduce the concentration of substrate metallic particles present in the MWCNTs. The attachment of amine group, carboxyl group, and ozone-treated MWCNTs was studied in order to ensure the homogeneous dispersion of the MWCNTs in matrix by Ma et al. [7]. Buang et al. [8] observed that the usage of acid-treated MWCNTs showed homogeneous dispersion and less defects on the side walls of MWCNTs compared to other functionalization techniques. Theodore et al. [9] studied the effect of various functionalized MWCNTs in

Table 1: Different methods for MWCNTs reinforcement.

Sample	MWCNTs wt.%	Acetone + MWCNTs	Epoxy + acetone	Removal of acetone after mixing
A-H 0.1	0.1	Tip sonication	Bath sonication	Hot air oven at 55°C
A-H 0.2	0.2	Tip sonication	Bath sonication	Hot air oven at 55°C
B-M 0.1	0.1	Tip sonication	Bath sonication	Magnetic stirring at 55°C
B-M 0.2	0.2	Tip sonication	Bath sonication	Magnetic stirring at 55°C
C-V 0.1	0.1	Tip sonication	Bath sonication	Vacuum oven at RT
C-V 0.2	0.2	Tip sonication	Bath sonication	Vacuum oven at RT

terms of thermal and mechanical properties. It was concluded that the attachment of –COOH group on the side walls of MWCNTs confirmed the enhancement of flexural strength and flexural modulus by 25.5 and 54.8%, respectively, for the 1 wt.% of reinforcement. Yu et al. [10] evaluated that the fracture toughness of epoxy reinforced with 1 and 3 wt.% of MWCNTs was found to be enhanced by 1.29 and 1.62 times, respectively. Similarly, the fatigue life was found to be enhanced by 9.3 and 10.5 times for the same MWCNTs concentration. Rahman et al. [11] optimized the mechanical properties of the epoxy reinforced with E-glass and amino-functionalized MWCNTs. The strength, Young's modulus, and strain at fracture of epoxy/E-glass/0.3 wt.% of MWCNTs were found to be enhanced by 37, 21, and 21%, respectively. It is observed from the previous studies that the functionalization of MWCNTs is very much essential in order to utilize the fullest potential of the reinforcement.

The thermal conductivity of the epoxy nanocomposites having 0.5 and 1 wt.% of silica-coated MWCNTs was found to be enhanced by 51 and 67%, respectively, by Cui et al. [12]. The interfacial bonding between epoxy and MWCNTs was also confirmed by the increase of thermal conductivity and broadening of the glass transition temperature (Tg) in the study by Pillai and Ray [13]. The MWCNTs were aligned in the epoxy resin to achieve the required properties by Park et al. [14], and the thermal conductivity of epoxy/MWCNTs nanocomposites at room temperature (RT) was observed to be 55 W/mK, and the stretched MWCNTs-epoxy sheet showed the value of 100 W/mK, whereas the same for pure epoxy was found to be 0.11 W/mK at RT.

Though different types of research works are going on in the field of epoxy-based nanocomposites, the homogeneous dispersion of reinforcement is yet to be achieved, and the unique way for the dispersion of MWCNTs in epoxy remains unfulfilled. Hence, an attempt is made to optimize the processing parameters in order to improve the mechanical and thermal properties of nanocomposites.

2. Materials and Methods

2.1. Materials. The MWCNTs were purchased from M/s Shenzhen Nanotech Port Co., Ltd., China. The specifications of as-received MWCNTs are as follows: outer diameter <10 nm, length 5–15 μm, purity 97%, ash content <3%, and specific surface area −250 to 300 m^2/g. Epoxy resin and hardener were received from M/s Endolite, India, Inc., having the density of 2.25 and 0.94 g/mL, respectively.

2.2. Chemical Treatment and Characterization of MWCNTs. The MWCNTs were functionalized using the acid treatment technique as suggested by Esumi et al. [15], which is briefly discussed here. The MWCNTs were dispersed in nitric and sulfuric acid mixture having the volume ratio of 1 : 3 and heated at 140°C in an oil bath with continuous mechanical stirring for 30 min. After the chemical treatment, MWCNTs were washed with distilled water until the pH value of the supernatant reached around 7. Then, the MWCNTs were dried in a hot air oven at 100°C. Thus, the chemically treated MWCNTs were obtained. The functional groups attached on the side walls of the MWCNTs were confirmed by the Fourier transform infrared spectroscopy (FTIR) technique. The concentration and types of functional groups present on the MWCNTs depend on the time of reflux and acid strength. Motchelaho et al. [16] reported that the peaks identified at 1360, 1710, and 3403 cm^{-1} were confirmed to be COO–, C=O, and –OH bonds, respectively, in the chemically modified MWCNTs. Peaks at 1710 and 3453 cm^{-1} were attributed to acidic groups like carbonyl, phenol, and lactol. Peak at 1576 cm^{-1} was assigned to C=C bond in MWCNTs. The defects in the MWCNTs after the chemical treatment were studied by the laser micro-Raman with 488 nm blue laser, where the defects were observed to be negligible.

2.3. Preparation of Nanocomposites. The resin and hardener having the weight ratio of 1 : 0.4 were hand-mixed using a stirrer rod for 15 min. and poured into the die having the dimension of 50 mm length and 9 mm diameter. Then, the mold was allowed to cure at 26 ± 2°C for 3 hrs, and, thus, the pure epoxy specimen was obtained. The nanocomposites having 0.1 and 0.2 wt.% of MWCNTs were prepared by three methods, and their detailed specifications are given in Table 1.

The epoxy resin was dissolved in acetone using bath sonication for 30 min., and the MWCNTs were dispersed in acetone using tip sonication for 30 min. Both were mixed together and bath-sonicated for another 45 minutes. Later, the acetone was removed using three methods, namely, hot air oven at 55°C (A), magnetic stirrer at 55°C (B), and under vacuum at room temperature (C). Then, the epoxy-MWCNTs mixture was mixed with required quantity of hardener by the hand mixing process for 15 min. and poured into the die. Thus, the nanocomposites were prepared once the mold was cured.

2.4. Characterization of Test Samples. The compression test of the sample was carried out as per ASTM D695 [17] using

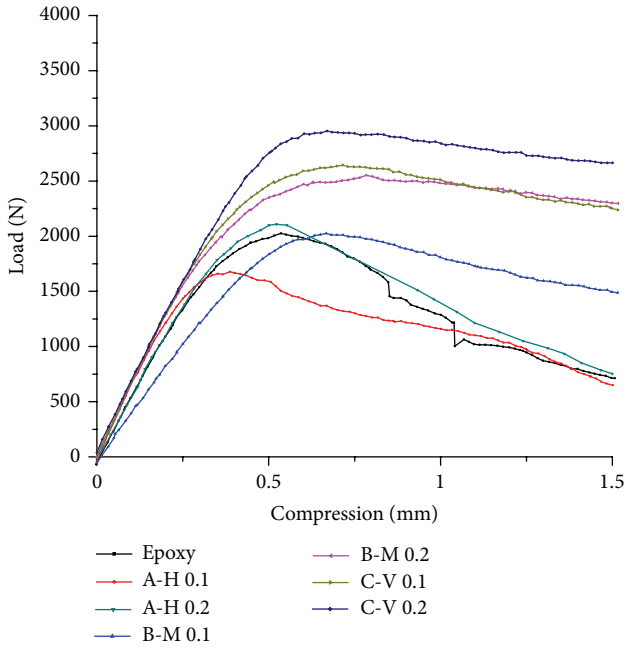

Figure 1: Load versus compression of epoxy nanocomposites.

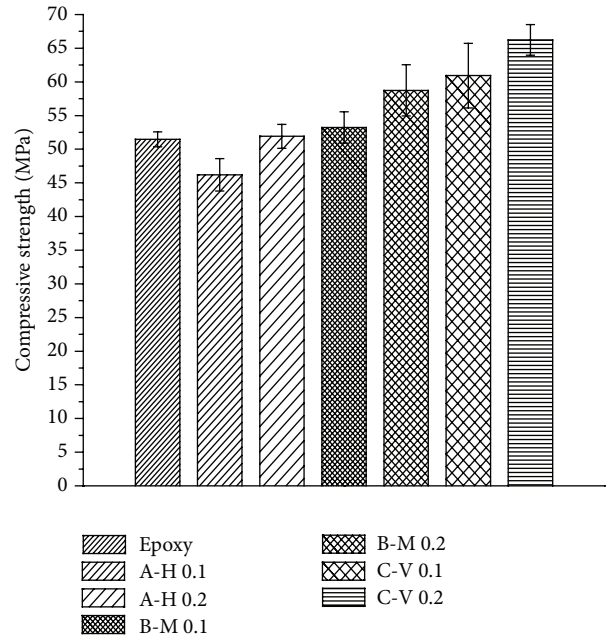

Figure 2: Compressive strength of nanocomposites.

a servo controlled closed loop Instron 8101. The thermal conductivity of the sample was measured by a KD2 Pro thermal properties analyzer using a dual-probe method. A Netzsch simultaneous thermal analyzer model STA 449 F3 having the DSC resolution of <1 μW and the microbalance resolution of <1 μg was used for calorimetric analysis of the test samples from room temperature to 800°C at a heating rate of 10 K/min. The test samples were prepared from the cured specimens weighing in the range of 5–10 mg. The sample chamber and the furnace chamber were purged with Ar gas before starting the test at 20 and 60 ml/min., respectively. In all cases, three specimens were tested, and the average of the results is reported. The homogeneous dispersion of the MWCNTs in epoxy was also confirmed by the same.

3. Results and Discussion

3.1. Mechanical Properties of Epoxy Nanocomposites. The load versus compression plots obtained for test samples processed by different methods are shown in Figure 1. It is observed that the strength of nanocomposites prepared by magnetic stirring and vacuum oven process was increased. However, it was found to be decreased for the sample prepared through hot air oven process compared to that of pure epoxy. It is also observed that the compressive strength of the nanocomposites was found to be increased with concentration of reinforcement irrespective of the processing technique followed.

The compressive strength (CS) and Young's modulus (EM) of test samples against processing conditions are shown in Figures 2 and 3, respectively. It is observed from Figures 2 and 3 that the CS and EM of epoxy were found to be increased with the reinforcement of MWCNTs. However, the CS and EM of A-H 0.1 were observed to be decreased by 11.4 and

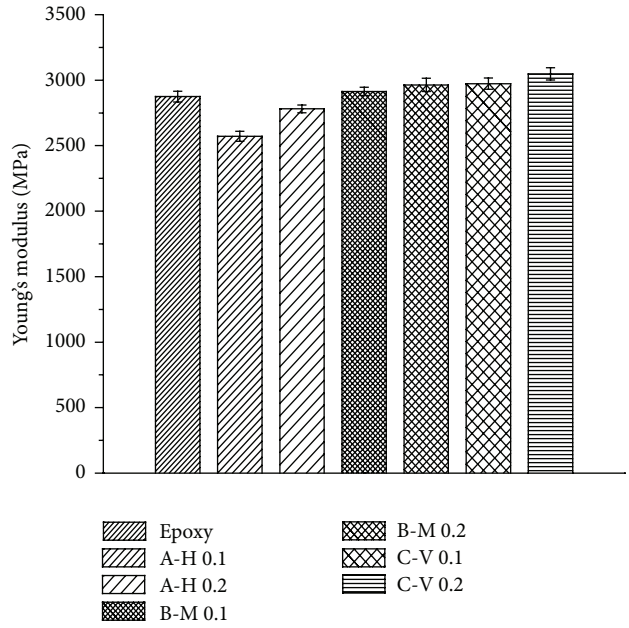

Figure 3: Young's modulus of the test samples.

11.8%, respectively, compared to those of pure epoxy. It is due to the fact that the method of removal of acetone by hot air oven led to destroying the chemical bonding between the MWCNTs and epoxy leading to decreased properties of nanocomposites. However, it was restricted when the MWCNTs' concentration was increased. Amount of heat supplied to evaporate the acetone was not sufficient enough to destroy the chemical bonding between them at 0.2 wt.% MWCNTs, and, thus, it led to the reduction of CS and EM by only 0.8 and 3.3%, respectively. The sample B-M

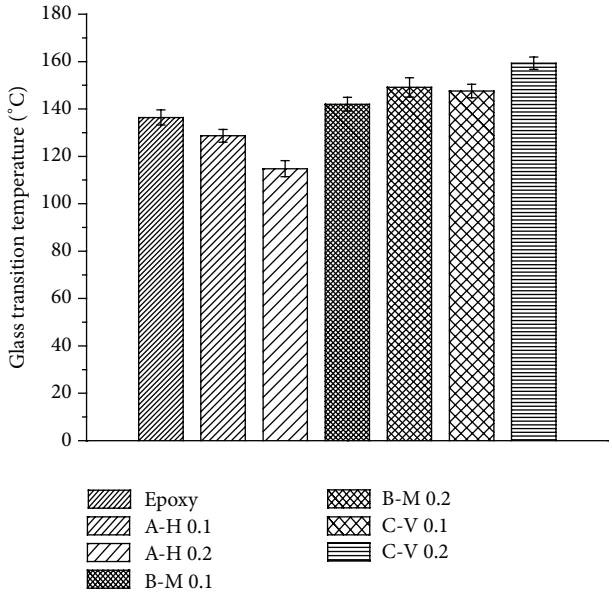

Figure 4: Glass transition temperature of the test samples.

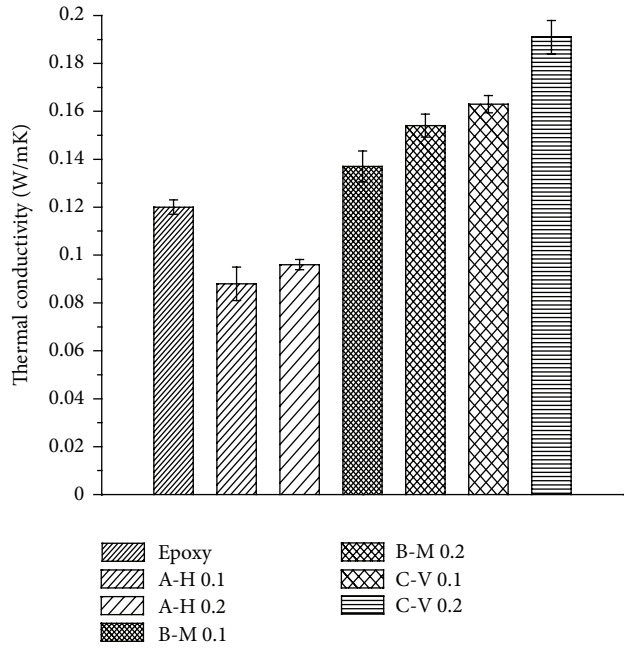

Figure 5: Thermal conductivity of nanocomposites.

0.2 showed the increase of CS and EM of nanocomposites by 14.2 and 3%, respectively, compared to those of pure epoxy resin. The enhancement of mechanical properties is due to the fact that the continuous stirring of the epoxy and MWCNTs in acetone reduced the debonding between them at the evaporation temperature of acetone, and it is expected to ensure the homogeneous dispersion of MWCNTs in epoxy. The sample C which used the vacuum oven for removing the acetone showed a significant enhancement in the mechanical properties compared to those of the samples A and B. During the vacuum condition at room temperature, the solvent was fully removed compared to the rest of the process. The enhancement of CS and EM of the C-V 0.2 sample was observed to be 39.4 and 10.7%, respectively, compared to pure epoxy. The observed enhancement of EM of epoxy with 0.1 wt.% MWCNTs was 3.4%, whereas it was reported to be only 2% for the same reinforcement condition by Starkova et al. [4]. The enhancement of mechanical properties of the nanocomposites was due to homogeneous dispersion of reinforcement and good interaction between the reinforcement and the matrix, which was also confirmed by Gojny and Schulte [18]. A strong physical network between MWCNTs and epoxy was confirmed by the shifting of glass transition temperature (Tg) of the nanocomposites, which is shown in Figure 4, leading to enhanced mechanical properties. The Tg of C-V 0.2 was observed to increase by 16.8% compared to that of pure epoxy confirming the previous observations. Guadagno et al. [19] confirmed the interaction between epoxy and MWCNTs with an increase of Tg and the homogeneous dispersion of the MWCNTs in epoxy. Pillai and Ray [13] confirmed the interaction between epoxy and MWCNTs with the broadening of Tg.

3.2. Thermal Conductivity and Stability of Epoxy Nanocomposites. Figure 5 shows the thermal conductivity of epoxy and its nanocomposites prepared by different processing conditions, It is observed that the thermal conductivity of the sample A-H 0.1 and A-H 0.2 was found to be 33.4% and 25%, respectively, lower than that of the pure epoxy, which is due to debonding between the reinforcement and the matrix. It is also observed that the thermal conductivity of samples B and C was found to be increased with the reinforcement of MWCNTs. The sample C showed significant enhancement of thermal conductivity compared to that of samples A and B. The enhancement of thermal conductivity is due to homogeneous dispersion of MWCNTs in epoxy resin and bonding between them. The enhancement of thermal conductivity was found to be 59.2% for C-V 0.2 compared to pure epoxy. The thermal stability of the sample was measured by the thermogravimetric analysis (TGA), and it is confirmed that the thermal stability of nanocomposites was improved significantly compared to that of pure epoxy, and it is shown in Figure 6. Venkata Ramana et al. [20] also observed the improved thermal stability of epoxy/MWCNTs nanocomposites compared to that of pure epoxy.

4. Conclusions

It is concluded that the compressive strength and Young's modulus of nanocomposites were found to be significantly increased for the specimens processed by vacuum drying at room temperature compared to any other method. An improved physical network between MWCNTs and epoxy was confirmed by the enhancement of thermal conductivity and the thermal stability. The Young modulus, compressive strength, and thermal conductivity of the vacuum oven processed sample at 0.2 wt.% of MWCNTs were found to be increased by 10.7, 39.4, and 59.2%, respectively, compared

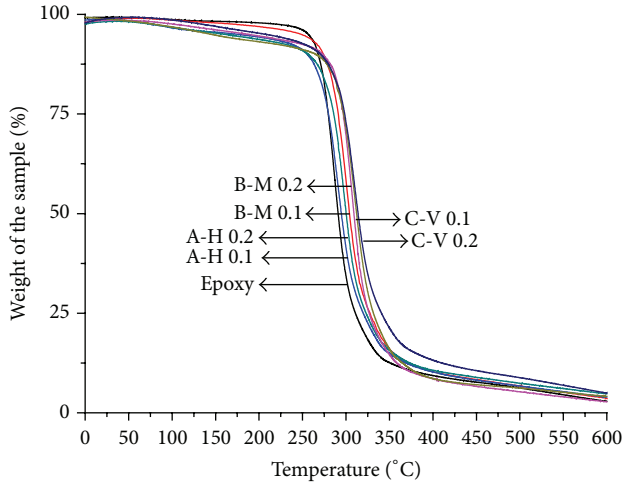

Figure 6: Thermal stability of nanocomposites.

to those of pure epoxy. Therefore, a unique method for the preparation of epoxy/MWCNTs nanocomposites is the solvent dispersion technique with vacuum drying process, where maximum enhancement of mechanical and thermal properties, homogeneous, dispersion of reinforcement in the matrix, and good interfacial bonding were obtained.

Abbreviations

MWCNTs:	Multiwalled carbon nanotubes
FTIR:	Fourier transform infrared spectroscopy
TGA:	Thermogravimetric analysis
DSC:	Differential scanning calorimetry
Tg:	Glass transition temperature
RT:	Room temperature
CS:	Compressive strength
EM:	Young's modulus.

Acknowledgments

Technical support given by the staff from the Material Science Lab, Central Instruments Facility, Strength of Materials Lab, and Advanced Manufacturing Lab of IIT Guwahati is highly acknowledged. Funding support given by DBT, India, through Project BT/233/NE/TBP/2011 is also acknowledged.

References

[1] F. H. Gojny, M. H. G. Wichmann, B. Fiedler, and K. Schulte, "Influence of different carbon nanotubes on the mechanical properties of epoxy matrix composites—a comparative study," *Composites Science and Technology*, vol. 65, no. 15-16, pp. 2300–2313, 2005.

[2] M.-F. Yu, B. S. Files, S. Arepalli, and R. S. Ruoff, "Tensile loading of ropes of single wall carbon nanotubes and their mechanical properties," *Physical Review Letters*, vol. 84, no. 24, pp. 5552–5555, 2000.

[3] M. Kim, Y.-B. Park, O. I. Okoli, and C. Zhang, "Processing, characterization, and modeling of carbon nanotube-reinforced multiscale composites," *Composites Science and Technology*, vol. 69, no. 3-4, pp. 335–342, 2009.

[4] O. Starkova, S. T. Buschhorn, E. Mannov, K. Schulte, and A. Aniskevich, "Creep and recovery of epoxy/MWCNT nanocomposites," *Composites A*, vol. 43, pp. 1212–1218, 2012.

[5] H. Mahfuz, S. Zainuddin, M. R. Parker, T. Al-Saadi, V. K. Rangari, and S. Jeelani, "Reinforcement of SC-15 epoxy with CNT/CNF under high magnetic field: an investigation of mechanical and thermal response," *Journal of Materials Science*, vol. 44, no. 4, pp. 1113–1120, 2009.

[6] L. He and S. C. Tjong, "Carbon nanotube/epoxy resin composite: correlation between state of nanotube dispersion and Zener tunneling parameters," *Synthetic Metals*, vol. 162, pp. 2277–2281, 2012.

[7] P.-C. Ma, S.-Y. Mo, B.-Z. Tang, and J.-K. Kim, "Dispersion, interfacial interaction and re-agglomeration of functionalized carbon nanotubes in epoxy composites," *Carbon*, vol. 48, no. 6, pp. 1824–1834, 2010.

[8] N. A. Buang, F. Fadil, Z. A. Majid, and S. Shahir, "Characteristic of mild acid functionalized multiwalled carbon nanotubes towards high dispersion with low structural defects," *Digest Journal of Nanomaterials and Biostructures*, vol. 7, no. 1, pp. 33–39, 2012.

[9] M. Theodore, M. Hosur, J. Thomas, and S. Jeelani, "Influence of functionalization on properties of MWCNT-epoxy nanocomposites," *Materials Science and Engineering A*, vol. 528, no. 3, pp. 1192–1200, 2011.

[10] N. Yu, Z. H. Zhang, and S. Y. He, "Fracture toughness and fatigue life of MWCNT/epoxy composites," *Materials Science and Engineering A*, vol. 494, no. 1-2, pp. 380–384, 2008.

[11] M. M. Rahman, S. Zainuddin, M. V. Hosur et al., "Improvements in mechanical and thermo-mechanical properties of e-glass/epoxy composites using amino functionalized MWCNTs," *Composite Structures*, vol. 94, pp. 2397–2406, 2012.

[12] W. Cui, F. Du, J. Zhao et al., "Improving thermal conductivity while retaining high electrical resistivity of epoxy composites by incorporating silica-coated multi-walled carbon nanotubes," *Carbon*, vol. 49, no. 2, pp. 495–500, 2011.

[13] S. K. Pillai and S. S. Ray, "Epoxy-based carbon nanotubes reinforced composites in advances," in *Nanocomposites—Synthesis, Characterization and Industrial Applications*, B. Reddy, Ed., pp. 727–792, 2011.

[14] J. G. Park, Q. Cheng, J. Lu et al., "Thermal conductivity of MWCNT/epoxy composites: the effects of length, alignment and functionalization," *Carbon*, vol. 50, no. 6, pp. 2083–2090, 2012.

[15] K. Esumi, M. Ishigami, A. Nakajima, K. Sawada, and H. Honda, "Chemical treatment of carbon nanotubes," *Carbon*, vol. 34, no. 2, pp. 279–281, 1996.

[16] M. A. M. Motchelaho, H. Xiong, M. Moyo, L. L. Jewell, and N. J. Coville, "Effect of acid treatment on the surface of multiwalled carbon nanotubes prepared from Fe-Co supported on $CaCO_3$: correlation with Fischer-Tropsch catalyst activity," *Journal of Molecular Catalysis A: Chemical*, vol. 335, no. 1-2, pp. 189–198, 2011.

[17] ASTM D 695-10., "Standard Test Method for Compressive Properties of Rigid Plastics," 2010.

[18] F. H. Gojny and K. Schulte, "Functionalisation effect on the thermo-mechanical behaviour of multi-wall carbon nanotube/epoxy-composites," *Composites Science and Technology*, vol. 64, no. 15, pp. 2303–2308, 2004.

[19] L. Guadagno, L. Vertuccio, A. Sorrentino et al., "Mechanical and barrier properties of epoxy resin filled with multi-walled carbon nanotubes," *Carbon*, vol. 47, no. 10, pp. 2419–2430, 2009.

[20] G. Venkata Ramana, B. Padya, R. Naresh Kumar, K. P. V. Prabhakar, and P. K. Jain, "Mechanical properties of multi-walled carbon nanotubes reinforced polymer nanocomposites," *Indian Journal of Engineering and Materials Sciences*, vol. 17, no. 5, pp. 331–337, 2010.